

1 Title:

2 **Variations in airborne bacterial communities at high altitudes over the Noto**
3 **Peninsula (Japan) in response to Asian dust events**

4

5 Authors:

6 Teruya Maki ^{*a}, Kazutaka Hara^b, Ayumu Iwata^c, Kevin C. Lee^d, Kei Kawai^e, Kenji Kai^e,
7 Fumihisa Kobayashi^f, Stephen B. Pointing^d, Stephen Archer^d, Hiroshi Hasegawa^a, and
8 Yasunobu Iwasaka^g

9

10 Author Affiliations:

11 ^a College of Science and Engineering, Kanazawa University, Kakuma, Kanazawa,
12 Ishikawa, 920-1192, Japan.

13 ^b National Institute for Environmental Studies, Tsukuba, Ibaraki 305-8506, Japan.

14 ^c Graduate school of Natural Science and Technology, Kanazawa University, Kakuma,
15 Ishikawa, 920-1192, Japan.

16 ^d School of Applied Sciences, Auckland University of Technology, Private Bag 92006,
17 Auckland 1142, New Zealand.

18 ^e Graduate School of Environmental Studies, Nagoya University; Furocho, Chikusaku,
19 Nagoya, 464-8601, Japan.

20 ^f Graduate School of Science and Technology, Hirosaki University, Bunkyo-cho 3,
21 Hirosaki, Aomori, 036-8561, Japan.

22 ^g Community Research Service Group, University of Shiga Prefecture, 2500
23 Yasakamachi, Hikoneshi, Shiga, 522-8533, Japan.

24

25 *Corresponding author:

26 Tel: +81-(0) 76-234-4793, Fax: +81-(0) 76-234-4800

27 E-mail: makiteru@se.kanazawa-u.ac.jp

28 **Abstract**

29 Aerosol particles, including airborne microorganisms, are transported through the
30 free troposphere from the Asian continental area to the downwind area in East Asia and
31 can influence climate changes, ecosystem dynamics, and human health. However, the
32 variations present in airborne bacterial communities in the free troposphere over
33 downwind areas are poorly understood, and there are few studies that provide an
34 in-depth examination of the effects of long-range transport of aerosols (natural and
35 anthropogenic particles) on bacterial variations. In this study, the vertical distributions
36 of airborne bacterial communities at high altitudes were investigated and the bacterial
37 variations were compared between dust events and non-dust events.

38 Aerosols were collected at three altitudes from ground level to the free troposphere
39 (upper level: 3,000 m or 2,500 m; middle level: 1,200 m or 500 m; and low level: 10 m)
40 during Asian dust events and non-dust events over the Noto Peninsula, Japan, where
41 westerly winds carry aerosols from the Asian continental areas. During Asian dust
42 events, air masses at high altitudes were transported from the Asian continental area by
43 westerly winds, and Laser Imaging Detection and Ranging (LIDAR) data indicated high
44 concentrations of non-spherical particles, suggesting that dust-sand particles were
45 transported from the central desert regions of Asia. The air samples collected during the
46 dust events contained 10–100 times higher concentrations of microscopic fluorescent
47 particles and Optical Particle Counter (OPC) measured particles than in non-dust events.
48 The air masses of non-dust events contained lower amounts of dust-sand particles.
49 Additionally, some air samples showed relatively high levels of black carbon, which
50 were likely transported from the Asian continental coasts. Moreover, during the dust

51 events, microbial particles at altitudes of >1,200 m increased to the concentrations
52 ranging from 1.2×10^6 particles m^{-3} to 6.6×10^6 particles m^{-3} . In contrast, when dust
53 events disappeared, the microbial particles at >1,200 m decreased slightly to
54 microbial-particle concentrations ranging from 6.4×10^4 particles m^{-3} to 8.9×10^5
55 particles m^{-3} .

56 High-throughput sequencing technology targeting 16S rRNA genes (16S rDNA)
57 revealed that the bacterial communities collected at high altitudes (from 500 m to 3,000
58 m) during dust events exhibited higher diversities and were predominantly composed of
59 natural-sand/terrestrial bacteria, such as *Bacillus* members. During non-dust periods,
60 airborne bacteria at high altitudes were mainly composed of anthropogenic/terrestrial
61 bacteria (Actinobacteria), marine bacteria (Cyanobacteria and Alphaproteobacteria), and
62 plant-associated bacteria (Gammaproteobacteria), which shifted in composition in
63 correspondence with the origins of the air masses and the meteorological conditions.
64 The airborne bacterial structures at high altitudes suggested remarkable changes in
65 response to air mass sources, which contributed to the increases in community richness
66 and to the domination of a few bacterial taxa.

67

68

69 **1. Introduction**

70 Airborne microorganisms (bioaerosols) associated with desert-sand and
71 anthropogenic particles were transported through free troposphere from the Asian
72 continents to downwind regions of East Asia and can influence climate changes,
73 ecosystem dynamics, and human health (Iwasaka et al., 2009). Natural dust events from
74 the Asian desert regions carry airborne microorganisms, supporting atmospheric
75 microbial dispersals (Griffin et al., 2007; Maki et al., 2010; Pointing and Belnap, 2014).
76 Haze days caused by anthropogenic particles from Asian continents also affect airborne
77 microbial abundance and endotoxin levels (Wei et al., 2016). Some studies
78 demonstrated that Asian dust events, including natural and anthropogenic particles,
79 cause vertical mixture of bioaerosols in downwind areas, such as in Japan (Huang et al.,
80 2015b; Sugimoto et al., 2012; Maki et al., 2015).

81 Bioaerosols, which include bacteria, fungi, and viruses, are transported from
82 ground environments to the free troposphere and account for a substantial proportion of
83 organic aerosols (Jaenicke, 2005). Bioaerosols are thought to influence atmospheric
84 processes by participating in atmospheric chemical reactions and in the formation of
85 cloud-nucleating particles (Pratt et al., 2009; Morris et al., 2011; Hara et al., 2016b).
86 Indeed, airborne microorganisms act as ice nuclei that are related to ice-cloud formation
87 processes (Möhler et al., 2007; Delort et al., 2010; Creamean et al., 2013; Joly et al.,
88 2013). In particular, ice-nucleation activating proteins of some microorganisms, such as
89 *Pseudomonas syringae*, *Xanthomonas campestris* and *Erwinia herbicola*, exhibit high
90 nucleation activities, initiating ice formation at relatively warm temperatures (greater
91 than -5 °C) (Morris et al. 2004) in comparison to the inorganic ice-nucleating particles,

92 such as potassium feldspar (approximately -8 °C) (Atkinson et al. 2013). Ice-nucleating
93 particles that originate from bioaerosols are believed to activate ice formation more
94 efficiently than inorganic substances (Hoose and Möhler, 2012; Murray et al. 2012), and
95 are primary contributors of rapid ice-cloud formation even at low concentrations in the
96 clouds at temperatures between -8 °C and -3 °C (Hallett and Mossop, 1974).
97 Bioaerosols are key factors for elucidating the detailed mechanisms of ice-cloud
98 formation and precipitation over East Asia (Hara et al., 2016ab), but the microbial
99 characteristics of bioaerosols transported over long distances by Asian-dust events are
100 still unclear. Furthermore, the microorganisms transported by Asian dust events increase
101 the allergenic burden, consequently inducing asthma incidences (Ichinose et al., 2005)
102 and contributing to the dispersal of diseases such as Kawasaki disease (Rodó et al.,
103 2011) and rust diseases (Brown and Hovmøller, 2002).

104 In downwind areas of East Asia, the atmospheric bacterial dynamics at high
105 altitudes should be investigated in order to understand the ecological and meteorological
106 influences of airborne bacteria as well as their long-range dispersion. Meteorological
107 shifts and dust events can dramatically alter airborne bacterial communities at high
108 altitudes in Japan (Maki et al., 2013 and 2015) because of air masses that originate from
109 heterogeneous environments, including marine, mountainous, urban, and desert areas.
110 The airborne microorganisms around North American mountains (2,700 m above sea
111 level) were also found to increase their species diversities in response to Asian dust
112 events (Smith et al., 2013). High-throughput sequencing technology can generate large
113 numbers of nucleotide sequences and the sequencing database has played an important
114 role for investigation of airborne bacterial compositions (Brodie et al., 2007; Woo et al.,

115 2013). Indeed, the analyses using high-throughput sequencing has demonstrated that
116 airborne bacterial populations at ground levels change in response to pollutants from
117 Beijing (Cao et al., 2014) and African dust events (Mazar et al., 2016). To investigate
118 their long-range transported bacteria while avoiding the ground-surface contaminations,
119 the bioaerosol samples collected at high altitudes by aircrafts were analyzed using
120 high-throughput sequencing, showing the airborne microbial diversities at high altitudes,
121 ranging from 1,000 m to 3,000 m (DeLeon-Rodriguez et al., 2013; Maki et al., 2015).
122 There are also a few studies on the vertical bacterial distribution from the ground level
123 to the troposphere (DeLeon-Rodriguez et al., 2013; Maki et al., 2015). Nonetheless,
124 while some variations were observed, the specific changes in tropospheric bioaerosols
125 over East Asia, and, in particular, differences between Asian dust and non-dust events
126 remain poorly understood.

127 Organic aerosol particles, such as bioaerosols, account for high rates of
128 tropospheric aerosols, ranging from 30 % to 80 % (Jaenicke, 2005), and fluctuate at
129 high concentrations, ranging from 10^3 to 10^5 particles m^{-3} , under the boundary layer at
130 4,000 m above the ground (Twohy et al., 2016). Epifluorescence microscopy using
131 fluorescent-dye staining is a useful tool for observation and determination of microbial
132 particles in the atmosphere, demonstrating that the biomass of airborne microorganisms
133 increased 10– to 100–fold during Asian-dust events (Hara et al., 2012, Maki et al.,
134 2014). Under a fluorescence microscope, DNA in microbial particles fluoresce blue
135 when stained with 4, 6-diamidino-2-phenylindole (DAPI) (Russell et al., 1974), and
136 organic materials aggregated with proteins and microbial cell components were
137 confirmed as yellow fluorescence particles (Mostajir et al., 1995). Mineral particles

138 (white particles) and black carbon (black particles) can also be observed as background
139 fluorescence in microscopic observation fields (Maki et al., 2014). Accordingly, several
140 DAPI-stained particles could be detected in air samples collected from all over Japan
141 during dust events (Maki et al., 2013) and can be used as indicators for evaluating the
142 amounts of some aerosol species during dust events.

143 In this study, the bacterial communities from different altitudes around the
144 Japanese islands were compared to identify the potential influences of long-range
145 transported air masses on tropospheric bacteria. We used a helicopter for collecting air
146 samples at altitudes ranging from 1,200 m to 3,000 m over the Noto Peninsula, Japan.
147 Helicopter sampling was used to collect chemical components at high altitudes, which
148 has previously been used to avoid contamination from the downwash created by
149 spinning rotors (Watanabe et al., 2016). This air sampling method can directly collect
150 aerosols moving from Asian continents or marine areas to Japan. We estimated the air
151 mass conditions using the meteorological data obtained during the sampling periods,
152 and determined aerosol amounts by using meteorological monitoring and
153 epifluorescence microscopic observation. Bacterial community structures were analyzed
154 by using high-throughput sequencing targeting bacterial 16S rRNA genes (16S rDNA).

155

156 **2. Experiments**

157

158 *2.1. Sampling*

159 Aerosol sampling using a helicopter (R44; Robinson, CA, USA) was performed
160 over coastal areas from Uchinada (36°67N, 136°64E) to Hakui (36°92N, 136°76E) in the

161 Noto Peninsula, Japan. Both cities are located on the western coast of the Noto
162 Peninsula where aerosols arrive from continental areas across the Sea of Japan and are
163 mixed with local aerosols (Fig. 1). The helicopter traveled 20 km northwest from
164 Kanazawa to Uchinada; air sampling was continuously conducted from Uchinada to the
165 northern coastal areas. To compare the vertical distributions of airborne bacteria during
166 dust and non-dust events, air samples were collected using a helicopter at the 1 to 3
167 altitudes ranging from 500 m to 3,000 m above ground level (Table 1). Air samples from
168 low altitude regions (10 m above ground level) were collected from the roof of a
169 building located at Taki bay in Hakui (36°92 N, 136°76 E). To compare the vertical
170 bacterial distribution, aerosol samples were collected during the daytime (from 9:00
171 Japanese standard time [JST; UTC + 9 h] to 16:30 JST) on March 19, 2013; April 28,
172 2013; March 28, 2014; and March 20, 2015. These samples were collected at the
173 following altitude sets; (1) 2,500 m, 1,200 m, and 10 m; (2) 3,000 m, 1,200 m, and 10
174 m; (3) 3,000 m, 1,200 m, and 10 m; and (4) 2,500 m and 500 m, respectively, and
175 samples were labeled as shown in Table 1. To investigate the bacterial changes at
176 altitudes in response to time, temporal transect at the altitude of 1,200 m was prepared
177 for seven days – the 23rd, 24th, 25th, and 29th of March 2014 and the 16th, 17th, and
178 21st of March 2015 – and the sample names are showed in Table 1.

179 Air samples were collected through sterilized polycarbonate filters (0.22- μ m pore
180 size; Whatman, Tokyo, Japan) with sterilized filter holders (Swinnex Filter holder;
181 Merck, Darmstadt, German) connected to an air pump. At the sterilization processes, the
182 filters and the filter-holder parts were irradiated separately under UV light for 1.0 h and
183 the filter holders attached with the filters were autoclaved at 121 °C for 20 min. Air

184 sampling was performed with a flow rates of 5 L min^{-1} over sampling periods from 0.2 h
185 to 1.0 h. Triplicate sampling filters were obtained for each altitude. During helicopter
186 sampling, outside air was transferred from a window to the bioaerosols-sampling inlet,
187 which was sterilized by autoclaving and UV irradiation. The sterilized filter holders
188 were inserted into the sampling inlet to avoid contamination. To collect air particles at
189 an altitude of 10 m, we used filter holders fixed on a 3 m stick, which was placed on the
190 roof of a building (Maki et al., 2014).

191 In total, 18 air samples were obtained during the sampling periods (Table 1). Of
192 the two filters used to collect each sample, one filter was used to determine the
193 particulate abundances under fluorescence microscopy, and the other was stored at
194 -80°C before the extraction of genomic DNA for analysis of bacterial compositions.

195

196 *2.2. Characteristics and trajectories of air masses*

197 Information regarding weather conditions (temperature, relative humidity, and
198 pressure) was gathered. During the helicopter flight, outside air was transferred from a
199 window into the meteorological-measurement inlet, into which the adaptor of the
200 measurement device (TR-73U; T&D Corporation, Matsumoto, Japan) was inserted, and
201 the temperature, relative humidity, and pressures were sequentially measured. The
202 temperature and relative humidity at an altitude of 10 m were also measured on the roof
203 of a building in Hakui. The depolarization ratio, which was measured by Laser Imaging
204 Detection and Ranging (LIDAR) measurements at Toyama, has been used for the
205 detection of non-spherical aerosols, such as mineral dust particles and/or sea salts.

206 To track the transport pathways of air masses, 72 h back trajectories were

207 calculated using the National Oceanic and Atmospheric Administration (NOAA)
208 HYbrid Single Particle Lagrangian Integrated Trajectory (HYSPLIT) model
209 (<http://www.arl.noaa.gov/HYSPLIT.php>). The coordinator of Hakui was used as the
210 back trajectory starting point at several altitudes from 10 m to 3,000 m above ground
211 level to estimate the trajectories of the air masses.

212

213 *2.3. Determination of particle abundance*

214 The air particles at each altitude were measured using an optical particle counter
215 (OPC: Rion, Tokyo, Japan). The OPC device was connected to the
216 meteorological-measurement inlet. The air particles at an altitude of 10 m were also
217 counted using the OPC device placed on the roof of a building.

218 Fluorescent particles stained with DAPI were also counted via epifluorescence
219 microscopy. Within 2 h of sampling, 1 mL of 1 % paraformaldehyde was added to one
220 of the filters to fix the aerosols. After a 1 h incubation, the filter was stained with DAPI
221 at a final concentration of 0.5 $\mu\text{g mL}^{-1}$ for 15 min (Russell et al., 1974). Next, the filter
222 was placed on a slide in a drop of low-fluorescence immersion oil (Type-F
223 IMMOIL-F30CC, Olympus, Tokyo, Japan). A second drop of oil was added, and a
224 coverslip was placed on top. Particles on the filter were observed using a fluorescence
225 microscope (BX-51, Olympus, Tokyo, Japan) with a UV excitation system. A filter
226 transect was scanned, and the four categorized particles, including white fluorescent
227 particles, blue fluorescent particles (microbial particles), yellow fluorescent particles,
228 and black particles, on the filter transect were counted using a previously reported
229 observational technique (Maki et al., 2014). The TA connections in DNA sequences of

230 microbial particles are bound with DAPI, emitting clear blue fluorescence. However, the
231 aggregation of organic matter might also accumulate DAPI at high amounts emitting
232 yellow fluorescence, which is due to formation of a compound with DAPI. Mineral
233 particles often have white autofluorescence or emit weak-blue (mostly white)
234 fluorescence originating from residues of DAPI on the particle surfaces and can be
235 identified on the weak blight background of microscopic observation fields. The black
236 color of black carbon can be identified in the background. The detection limit of aerosol
237 particle concentration was 1.1×10^4 particles m^{-3} of air.

238

239 *2.4. Analysis of bacterial community structures using MiSeq sequencing analysis*
240 *targeting 16S rDNA sequences*

241 After the aerosol particles on the other two filters were suspended in 3 mL of
242 sterile 0.6 % NaCl solution, the particles were pelleted by centrifugation at $20,000 \times g$
243 for 10 min. The genomic DNA (gDNA) was then extracted from the particle pellets
244 using sodium dodecyl sulfate, proteinase K, and lysozyme and purified by
245 phenol-chloroform extraction as previously described (Maki et al., 2008). The bacterial
246 community structure was determined using MiSeq DNA sequencing, which facilitates
247 multiplexed partial sequencing of 16S rDNA. Fragments of 16S rDNA (approximately
248 500 bp) were amplified from the extracted gDNA by PCR using the universal 16S
249 rDNA bacterial primers 515F (5'- Seq A -TGTGCCAGCMGCCGCGGTAA-3') and
250 806R (5'- Seq B -GGACTACHVGGGTWTCTAAT-3') (Caporaso et al., 2011), where
251 Seq A and Seq B represent the nucleotide sequences bounded by the second set of PCR
252 primers described below. The PCR amplicon sequences covered the variable region V4

253 of the 16S rRNA gene. Thermal cycling was performed using a thermocycler (Program
254 Temp Control System PC-700; ASTEC, Fukuoka, Japan) under the following
255 conditions: denaturation at 94°C for 1 min, annealing at 52°C for 2 min, and extension
256 at 72°C for 2 min for 20 cycles. Fragments of 16S rDNA in PCR products were
257 amplified again using the second PCR forward primer (5'- Adaptor C - xxxxxxxx - Seq
258 A -3') and reverse primer (5'- Adaptor D - Seq B -3'), where Adaptors C and D were
259 used for the Miseq sequencing reaction. The sequences "xxxxxxx" comprise an 8
260 nucleotide sequence tag designed for sample identification barcoding. Thermal cycling
261 was performed under the following conditions: denaturation at 94°C for 1 min,
262 annealing at 59°C for 2 min, and extension at 72°C for 2 min for 15 cycles. PCR
263 amplicons were purified using the MonoFas DNA purification kit (GL Sciences, Tokyo,
264 Japan). PCR amplicons from each sample were pooled at approximately equal amounts
265 into a single sequencing tube on a MiSeq Genome Sequencer (Illumina, CA, USA)
266 machine. The sequences obtained for each sample were demultiplexed based on the tag,
267 including the 8 nucleotide sequence. After removal of the tags, an average read length of
268 450 bp was obtained. Negative controls (no template and extraction products from
269 unused filters) were prepared in the DNA extraction process to check for contamination.
270 The amount of gDNA extracted from air samples ranged from the detection limit (<0.5
271 ng/samples) to approximately 50 ng/samples and cannot be determined directly by light
272 absorbance measurements. Accordingly, quantities of gDNA were estimated using the
273 PCR products after the first amplification step, and compared with the
274 microbial-particle concentrations that were determined by fluorescence microscopic
275 observation. The efficiency of the gDNA extraction from air samples was more than

276 80 %.

277 Before the analysis of bacterial community structures, USEARCH v.8.01623
278 (Edgar, 2013) was used to process the raw Illumina sequencing reads. Anomalous
279 sequences were removed with the following workflow. First, the forward and reverse
280 paired-end reads were merged, and the merged reads with lengths outside of the
281 200-500 bp range or those exceeding 6 homopolymers were discarded using Mothur
282 v1.36.1 (Schloss et al., 2009). Next, the sequences were subjected to Q-score filtering to
283 remove reads with more than one expected error. Reads occurring only once in the
284 entire dataset (singleton) were then removed. These sequences were clustered *de novo*
285 (with a minimum identity of 97 %) into 204 operational taxonomic units (OTUs) among
286 the 18 samples. The taxonomy of the representative OTU sequences was assigned using
287 the RDP classifier (Wang et al., 2007) implemented in QIME v1.9.1 (Caporaso et al.,
288 2010). Non-metric multidimensional scaling (NMDS) plot of the pairwise Bray-Curtis
289 distance matrix were used for the classification of all air samples. Greengenes release
290 13_8 (McDonald et al., 2012) was used as the reference taxonomic database.

291

292 2.5. Accession numbers

293 All data obtained from MiSeq sequencing data have been deposited in the
294 DDBJ/EMBL/GenBank database (accession number of the submission is
295 PRJEB17915).

296

297 **3. Results**

298

299 *3.1. Air mass analyses using LIDAR measurements, back trajectories, and metrological*
300 *data*

301 The vertical distributions of the depolarization ratio determined by LIDAR
302 measurements were assessed for the four sampling events (March 19, 2013; March 20,
303 2015; April 28, 2013; and March 28, 2014). The depolarization ratio increased at the
304 altitude of 3,000 m on March 19, 2013 (Fig. 2a), while it decreased at the middle
305 altitude of 1,000 m. The air mass on March 20, 2015 showed high values of
306 depolarization ratio at altitudes of 2,500 m and 500 m, consistent with the vertical
307 distribution of non-spherical (mineral dust) particles over the Noto Peninsula (Fig. 2d).
308 A 3-day back trajectory analysis indicated that the air mass at 3,000 m on both sampling
309 dates came from the Asian desert region to the Noto Peninsula (Hakui) immediately
310 across the Sea of Japan (Fig. 3). These results indicated the dust event occurrence on
311 March 19, 2013 was specific to the upper altitude of 3,000 m, while the dust event on
312 March 20, 2015 occurred between the altitudes of 2,500 m and 500 m. Moreover,
313 samples collected on April 28, 2013 and March 28, 2014 exhibited low depolarization
314 ratio (Fig. 2b-c), and the air masses on these two sampling dates came from areas of
315 North Asia, including eastern Siberia (Fig. 3).

316 The air-sampling periods from the March 2014 time series (from the 23rd to the 29th
317 of March 2014) and the March 2015 time series (from the 16th to the 21st of March
318 2015) showed different patterns of depolarization ratio and air mass trajectory roots
319 between the two series (Figs. 4 and 5). Depolarization ratio from March 2014
320 maintained lower values (Fig. 4a) and the trajectory lines changed the roots from eastern
321 Siberia to the Korean Peninsula before surrounding the Japanese islands (Fig. 4c). In

322 contrast, the sampling period during March 2015 had substantially higher depolarization
323 ratio, indicating a strong presence of mineral dust particles (Fig. 5a), and air masses at
324 3,000 m consistently originated from the Asian desert regions (Fig. 5c).

325 Temperatures from March 19, 2013; April 28, 2013; March 28, 2014; and March 20,
326 2015 increased from approximately 290 K to approximately 300 K at middle altitudes
327 (500 m and 1,200 m) (Fig. 2). The temperature profile clearly indicated the presence of
328 a thin boundary under the upper altitudes (2,500 m and 3,000 m), which suggested that
329 there is a difference in air qualities between the middle and upper altitudes (Table 1).

330 During the March 2014 time series, temperatures dynamically changed at altitudes of
331 approximately 1,200 m, while those from the March 2015 time series (the 16th, 17th,
332 and 21st of March 2015) were stable at 1,200 m (Figs. S1 and S2). These results
333 indicate that the boundary layers were located at 1,200 m during the March 2014 time
334 series, whereas the tropospheric air transported by westerly winds was suspended at the
335 sampling altitudes (500 m and 1,200 m) used during the March 2015 time series.

336

337 *3.2. Vertical distributions and sequential variations of aerosol particles*

338 Aerosol particle concentrations from the ground level to the troposphere were
339 measured using OPC to compare the vertical distributions of aerosols from the four
340 sampling events. The OPC-measured particles on March 19, 2013 and March 20, 2015
341 maintained similar concentrations below the troposphere (Fig. 2ad), while the
342 concentrations on April 28, 2013 and March 28, 2014 decreased one or two orders of
343 magnitude between the troposphere and ground level (Fig. 2bc). At high altitudes (2,000
344 m to 2,500 m), the coarse particles (greater 1.0 μm) observed on March 19, 2013 and

345 March 20, 2015 were one or two orders of magnitude higher (10^5 to 10^6 particles m^{-3})
346 than those on April 28, 2013 and March 28, 2014 (no more than 1.2×10^4 particles m^{-3}).
347 The fine particles ($0.3 \mu m$ to $1.0 \mu m$) showed similar concentrations between the four
348 sampling events, fluctuating between 1.2×10^6 to 3.5×10^7 particles m^{-3} . At lower
349 altitudes (130 m to 510), the aerosol particles had similar concentrations and size
350 distributions between the four sampling periods; the coarse particle concentration
351 ranged from 8.4×10^5 particles m^{-3} to 1.2×10^6 particles m^{-3} , and the fine particles
352 ranged from 1.3×10^7 particles m^{-3} to 1.2×10^8 particles m^{-3} .

353 OPC measurements indicated that air samples collected at 1,200 m during the March
354 2015 time series consistently contained coarse particles at one or two orders of
355 magnitude higher in concentration (1.4×10^6 to 3.4×10^6 particles m^{-3}) than detected in
356 the March 2014 time series, which had concentrations of no more than 1.8×10^5
357 particles m^{-3} (Fig. 4b). The concentration of relatively large particles ($>5.0 \mu m$) in
358 March 2015 maintained relatively higher concentrations (from 1.4×10^4 to 8.2×10^5
359 particles m^{-3}) than those observed in March 2014 (no more than 3.74×10^3 particles m^{-3}).
360 In contrast, the fine particles measured in March 2014 and March 2015 fluctuated
361 around similar concentrations ranging from 10^7 to 10^8 particles m^{-3} .

362 Based on the above observations, the sampled air masses that were influenced by
363 Asian dust events and included dust particles were categorized as “dust samples”. The
364 sampled air masses that were not influenced by dust events or contained less dust
365 particles were categorized as “non-dust samples”, in relation to the presence or absence
366 of dust events as the source of the aerosol samples (Table 1).

367

368 *3.3. Fluorescent microscopic observation of aerosol particles*

369 Using epifluorescence microscopy with DAPI staining, the aerosol particles in the
370 18 air samples emitted several types of fluorescence, categorized as white, blue, yellow,
371 or black (Fig. S3). White fluorescence particles, (white particles) were indicative of
372 mineral particles originating from the sand or soil. Microbial (prokaryotic) particles
373 stained with DAPI emitted blue fluorescence, forming coccoid- or bacilli-like particles
374 with a diameter $<3 \mu\text{m}$. Yellow fluorescence particles (yellow particles) stained with
375 DAPI were organic matter and ranged from $1.0 \mu\text{m}$ to $10 \mu\text{m}$ in diameter. Most of the
376 yellow particles disappeared in the aerosol-particle suspending solutions after protease
377 treatment, suggesting that the yellow particles consisted mainly of proteins. Black
378 particles were indicative of an anthropogenic black carbon originating from East Asian
379 regions, produced by biomass burning, industrial activities, and vehicle exhaust.

380 The dust samples from upper altitudes (2,500 m and 3,000 m) contained 5 to 100
381 times higher concentrations of microbial, organic, and white particles than the
382 concentrations detected in the non-dust samples (Fig. 2). In the upper altitude dust
383 samples, the concentration of mineral particles ranged from $7.77 \times 10^5 \text{ particles m}^{-3}$ to
384 $1.08 \times 10^6 \text{ particles m}^{-3}$ (Fig. 2ad), whereas the concentrations of the non-dust samples
385 ranged from $3.14 \times 10^4 \text{ particles m}^{-3}$ to $1.48 \times 10^5 \text{ particles m}^{-3}$ (Fig. 2bc). The
386 microbial particles in the high altitude dust samples exhibited concentrations of
387 approximately $1.5 \times 10^6 \text{ particles m}^{-3}$ that were two orders of magnitude higher than in
388 the non-dust samples (approximately $6.0 \times 10^4 \text{ particles m}^{-3}$). The organic particles in
389 the high altitude dust samples were also found at higher concentrations of
390 approximately $4.2 \times 10^6 \text{ particles m}^{-3}$ than those from the non-dust samples 13H428-u

391 and 14H328-u, which were 2.12×10^4 particles m^{-3} and 5.30×10^4 particles m^{-3} ,
392 respectively. In contrast, the air samples collected at the low altitude of 10 m exhibited a
393 random or stochastic pattern between 10^5 and 10^6 particles m^{-3} , regardless of the
394 sampling dates (Fig. 2). Black particles were observed in the four air samples from 10 m
395 and fluctuated around concentrations of less than 8.48×10^4 particles m^{-3} . Finally, the
396 percentage of organic particles out of the total number of particles (organic and
397 microbial particles) in the dust samples 13H319-u, 15H320-u, and 15H320-m ranged
398 between approximately 71.5 % and 73.6 %, which was higher than in the non-dust
399 samples, which ranged from 4.6 % to 46.3 % (Fig. S4).

400 All types of fluorescence particles were also observed in the sequentially collected
401 air samples at 1,200 m in the March 2015 time series (except for 2,500 m on March
402 20th) and the March 2014 series. The dust samples examined from the March 2015
403 series had higher concentrations of total particles than the non-dust samples of the
404 March 2014 series (Figs. 4 and 5). The mineral particles detected in the March 2014
405 series fluctuated at low concentrations from 3.39×10^4 particles m^{-3} to 2.62×10^5
406 particles m^{-3} (Fig. 4), while in the March 2015 series the mineral particles showed
407 higher values from 1.80×10^5 particles m^{-3} to 1.77×10^7 particles m^{-3} (Fig. 5). High
408 levels of organic particles were detected in the March 2015 series samples, ranging from
409 3.13×10^5 to 3.75×10^7 particles m^{-3} , which decreased to below 2.28×10^5 particles m^{-3}
410 in the March 2014 series samples. The microbial particle concentrations in the March
411 2015 series samples (ranging from 4.75×10^5 to 2.06×10^6 particles m^{-3}) were higher
412 than those of in the March 2014 series samples (ranging from 3.31×10^5 to 1.25×10^6
413 particles m^{-3}). The ratio of organic particles to the total number of organic and microbial

414 particles detected during March 2015 (71.5 % to 95.6 %) were higher than those during
415 March 2014 series (8.0 % to 36.2 %) (Fig. S4). The black particles were randomly
416 observed in all samples from March 2015 and March 2014.

417

418 *3.4. Analysis of bacterial communities using MiSeq sequencing analysis*

419 For the analysis of the prokaryotic composition in the 18 samples, we obtained
420 645,075 merged paired-end sequences with the lengths ranging from 244 bp to 298 bp
421 after quality filtering, and the sequence library size for each sample was normalized at
422 1,500 reads. The 16S rDNA sequences were divided into 204 phylotypes (sequences
423 with >97 % similarity). Phylogenetic assignment of sequences resulted in an overall
424 diversity of 16 phyla and candidate divisions, 32 classes (and class-level candidate taxa),
425 and 72 families (and family-level candidate taxa). The majority (>90 %) of the
426 sequences were represented by 9 bacterial classes and 33 families (Figs. 6 and 7). The
427 bacterial compositions varied during the sampling periods and included the phylotypes
428 belonging to the classes Cyanobacteria, Actinobacteria, Bacilli, Bacteroidetes, SBRH58,
429 and Proteobacteria (Alpha, Beta, Gamma, and Deltaproteobacteria), which are typically
430 generated from atmospheric, terrestrial and marine environments. On the box plots, the
431 numbers of bacterial species estimated by Chao I were similar at average levels between
432 the dust samples and non-dust samples, while the Chao I and Shannon values of the
433 non-dust samples showed a wider range than that of dust samples (Fig. 8a). A
434 non-metric multidimensional scaling (NMDS) plot demonstrated the distinct clustering
435 of prokaryotic communities separating the dust samples and the non-dust samples (Fig.
436 8b). For the PCR-analysis steps, negative controls (no template and template from

437 unused filters) did not contain 16S rDNA amplicons demonstrating the absence of
438 artificial contamination during experimental processes.

439

440 *3.5. Vertical distributions of bacterial communities in dust and non-dust samples*

441 The vertical distributions of bacterial compositions showed different patterns
442 between dust event days and non-dust days (Fig. 6). In the dust samples collected at
443 upper altitudes, phylotypes belonging to the phylum Bacilli accounted for more than
444 60.5 % of the total and were mainly composed of members of the families Bacillaceae
445 and Paenibacillaceae (Fig. 6). Bacterial numbers from the phylum Bacilli decreased at
446 lower altitudes during dust events, and the phylotypes of Cyanobacteria, Actinobacteria,
447 and Proteobacteria increased in relative abundance in the samples collected at middle and
448 low altitudes (13H319-m, 13H319-l, and 15H320-m).

449 Cyanobacteria, Actinobacteria, and Proteobacteria sequences also dominated in the
450 air samples collected during non-dust events (13H428-m, 14H328-u, 14H328-m, and
451 14H328-l). Specifically, Actinobacteria phylotypes increased in their relative abundance,
452 ranging from 14.1 % to 24.7 % in the non-dust samples collected on March 28, 2014.
453 Proteobacteria phylotypes containing several bacterial families occupied a high relative
454 abundance, ranging from 60.5 % to 85.3 % in the non-dust samples 13H428-u,
455 13H428-m, 14H328-u, 14H328-m, and 14H328-l. In particular, the non-dust samples
456 collected on March 28, 2014 included the Alphaproteobacteria phylotypes, which have
457 composed of members of the families Phyllobacteriaceae and Sphingomonadaceae.
458 Most Betaproteobacteria, phylotypes including the families Oxalobacteraceae and
459 Comamonadaceae, were specific to the non-dust samples collected at 1,200 m and 2,500

460 m on April 28, 2013.

461 Cyanobacteria phylotypes, which were randomly detected from both dust samples
462 and non-dust samples, particularly increased in both the non-dust sample collected at 10
463 m on April 28, 2013 and the dust sample collected at 3,000 m on March 20, 2015, with a
464 relative abundance of 15.3 % and 74.6 %, respectively. Bacteroidia phylotypes also
465 randomly appeared in several air samples, regardless of the dust event influences and
466 were present at maximal levels in the non-dust sample 13H319-m, with a relative
467 abundance of 35.6 %.

468

469 *3.6. Variations in bacterial communities during dust events and non-dust events*

470 Sequential variations in the bacterial composition of air samples at altitudes of
471 1,200 m or 2,500 m were compared between dust event periods (March 2015 series) and
472 non-dust periods (March 2014 series). During the March 2015 dust event, phylotypes of
473 the family Bacillaceae in the class Bacilli occupied more than 53.0 % of the relative
474 abundance in the four dust samples collected (Fig. 7). Cyanobacteria phylotypes related
475 to the marine cyanobacterium Synechococcaceae uniquely appeared in the dust samples
476 of the March 2015 series; their abundance fluctuated the values ranging from 12.5 % to
477 14.8 % between the 16th and the 20th of March 2015 before decreasing to 1.5 % on
478 March 20.

479 During the non-dust periods of the March 2014 series at the middle altitude, the
480 relative abundance of Actinobacteria phylotypes belonging to the family
481 Micrococcaceae was occupied 59.9 % on March 23, decreased to 19.5 % on March 24,
482 and disappeared from samples collected on March 29. Corresponding to the decrease in

483 Actinobacteria phylotypes, Alpha and Gammaproteobacteria phylotypes showed an
484 increasing trend from 30.6 % to 96.8 % between the 23rd and the 29th of March 2014
485 (Fig. 7a). Alphaproteobacteria phylotypes belonging to the families Sphingomonadaceae,
486 and Phyllobacteriaceae, consistently appeared throughout the sampling periods of the
487 March 2014 series and occupied a maximum relative abundance of 72.9 % and 22.3 %
488 respectively. For Gammaproteobacteria, the Xanthomonadaceae sequences dominated at
489 a relative abundance of 18.3 % and 5.4 % in the non-dust samples 14H325-m and
490 14H329-m, respectively, during the air mass was suspended the Japanese islands for a
491 few days.

492

493 **4. Discussion**

494

495 *4.1 Air mass conditions during Asian dust and non-dust events*

496 Westerly winds blowing over East Asia disperse airborne microorganisms
497 associated with dust mineral particles (Maki et al., 2008) and anthropogenic particles
498 (Cao et al., 2014; Wei et al., 2016), influencing the abundances and taxon compositions
499 of airborne bacteria at high altitudes over downwind areas, such as Noto Peninsula
500 (Maki et al., 2013). In this investigation, the increases in aerosol particles (dust
501 particles) and associated microbial particles were observed over the Noto Peninsula
502 during the dust events of March 19, 2013 and March 20, 2015 (Figs. 2 and 4). At the
503 two sampling dates, the air mass including microbial particles had traveled from the
504 Asian desert region throughout the anthropogenic polluted areas (Fig. 2), and the dust
505 particles entered the Japanese troposphere and were maintained at high altitudes (March

506 19, 2013) or mixed with the ground-surface air (March 20, 2015). During non-dust days,
507 the air masses at high altitudes came from several areas, including the eastern region of
508 Siberia, Asian continental coasts (Korean Peninsula), the Sea of Japan, or surrounding
509 Japanese islands, and mixed with ground-surface air over the Noto Peninsula. The air
510 samples collected during dust and non-dust events were valuable for understanding the
511 westerly wind influences on vertical distributions and sequential dynamics of airborne
512 bacteria at high altitudes over the downwind regions.

513

514 *4.2 Aerosol dynamics during Asian dust and non-dust event*

515 The microscopic fluorescence particles of all samples could be separated into four
516 categories: mineral (white), microbial (blue), organic (yellow), and black-carbon (black)
517 particles (Fig. S3), which were observed in the previous air samples collected during
518 dust events (Maki et al., 2015). The amount of microbial particles increased at high
519 altitudes during dust events, suggesting that the dust events directly carried bacterial
520 particles to the troposphere over downwind areas. At low altitudes, similar
521 concentrations of fluorescent particles were observed in air samples collected between
522 dust events (13H319-1) and non-dust events (13H428-1) (Fig. 2) because the dust
523 particles did not reach the ground surface on the dust-event days. In the absence of the
524 influences of dust-events, the aerosols mainly originated from local environments in
525 Japanese areas.

526 Organic particles also increased during dust events and in the ratios between all
527 particles related to the dust events. The organic particles originate from proteins and
528 other biological components (Mostajir et al., 1995). The tropospheric aerosols would be

529 composed of organic particles at high rates ranging from 30 % to 80 % (Jaenicke, 2005),
530 and organic particle concentrations fluctuated from 10^3 to 10^5 particles m^{-3} at high
531 altitudes of 4,000 m above the ground (Twohy et al., 2016). The dead-phase cells of
532 microbial isolates obtained from aerosol samples mainly irradiated yellow fluorescence
533 instead of blue fluorescence (Liu et al., 2014). When fungi (*Bjerkandera adusta*) and
534 bacteria (*Bacillus* spp.) isolated from aerosol samples were incubated, the dead-phase
535 microbial cells mainly irradiated yellow fluorescence instead of blue fluorescence (Liu
536 et al., 2014; Fig. S3). The relative numbers of organic particles to the total number of
537 microbial and organic particles in the dust samples showed significantly higher values
538 (82.9 ± 32.3 %) than in the non-dust samples (23.3 ± 13.7 %) (Fig. S4). Hara and Zhang
539 reported that dust events in Kyushu, Japan, resulted in an increased ratio of damaged
540 microbial cells in the air at the ground-surface and that the ratio increased to
541 approximately 80 % (Hara and Zhang, 2012). Furthermore, organic molecules
542 associated with dust aerosols are reported to be composed of mannitol, glucose, and
543 fructose, which are part of cell components of airborne microorganisms and contribute
544 to the formation of secondary organic aerosols (SOA) (Fu et al., 2016). Microbial cells
545 or their components coming from Asian continents to Japan would be exposed to air at
546 high-altitudes during their long-range transport, increasing the ratios of damaged and
547 dead cells or SOA.

548 The appearance of black carbon most likely originated from anthropogenic
549 activities, such as biomass burning, industrial activities, and vehicle exhaust (Chung and
550 Kim, 2008). In the anthropogenic regions of eastern China, anthropogenic particles
551 originating from human activities are expected to comprise more than 90 % of dust

552 particles (Huang et al., 2015a). When the westerly winds are strongly blowing over the
553 Noto Peninsula, the black carbon particles at upper altitudes (3,000 m) are thought to
554 mainly derive from continental anthropogenic regions.

555

556 *4.3 Comparing the community structures of atmospheric bacteria between Asian dust* 557 *and non-dust events*

558 Dust events and air-pollutant occurrences changed the airborne bacterial
559 communities over the downwind areas, such as Beijing (Jeon et al., 2011; Cao et al.,
560 2014) and east Mediterranean areas (Mazar et al., 2016). The westerly winds blowing
561 over East Asia would transport airborne bacteria to the high-altitude atmosphere over
562 the Noto Peninsula (Maki et al., 2015) and North American mountains (Smith et al.,
563 2013). Our box plots analysis suggested that changes in the bacterial diversity in the
564 dust samples would be more stable than in the non-dust samples (Fig. 8a). Furthermore,
565 using a NMDS plot, the bacterial compositions in the dust samples could be
566 distinguished from non-dust samples (Fig. 8b). Thus, the aerosol particles transported
567 by Asian dust events changed the atmospheric bacterial composition at higher altitudes
568 over downwind areas.

569 The phylotypes in the dust samples were predominately clustered into the class
570 Bacilli (Fig. 4a), while the non-dust samples mainly included the phylotypes of the
571 classes Alpha, Beta, and Gammaproteobacteria and Actinobacteria. Our previous
572 investigations indicated that the bacterial communities at an altitude of 3,000 m over the
573 Noto Peninsula included more than 300 phylotypes, which were predominantly
574 composed of Bacilli phylotypes (Maki et al., 2015). Bacterial groups belonging to

575 Bacilli, Proteobacteria, and Actinobacteria have been reported as airborne bacteria
576 around European mountains (Vařtilingom et al., 2012) as well as over Asian rural
577 regions (Woo et al., 2013). Some Bacilli isolates were found to act as ice-nucleating
578 agents and to be involved in ice cloud (Matulova et al., 2014; Mortazavi et al., 2015).
579 Isolates of Gammaproteobacteria isolates were obtained from mineral dust particles
580 (Hara et al., 2016a), glaciated high-altitude clouds (Sheridan et al., 2003), and plant
581 bodies (Morris et al., 2008), and some isolate species, such as *Pseudomonas*, were
582 confirmed to have the ice-nucleation activity. Accordingly, Bacilli and Proteobacteria
583 members associated with dust events could potentially contribute to climate change
584 resulting from dust events.

585

586 *4.4 Dominant bacterial populations in the air masses transported from Asian continents*

587 In some dust-event samples collected at high altitudes (13H319-u, 15H320-u, and
588 15H320-m), Bacilli sequences accounted for more than 52.7 % of the total number of
589 sequences (Fig. 6). Back trajectories on March 19, 2013 and March 20, 2015 came from
590 the Asian desert region to the Noto Peninsula. Some *Bacillus* species were
591 predominantly detected at high altitudes above the Taklimakan Desert (Maki et al.,
592 2008) and above downwind areas during Asian dust events (Maki et al., 2010 and 2013;
593 Smith et al., 2013; Jeon et al., 2011; Tanaka et al., 2011). *Bacillus* species are the most
594 prevalent isolates obtained from mineral dust particles collected over downwind areas
595 (Hua et al., 2007; Gorbushina et al., 2007).

596 Bacilli members can form resistant endospores that support their survival in the
597 atmosphere (Nicholson et al., 2000). The *Bacillus* isolates obtained from atmospheric

598 samples showed higher-level resistance to UV irradiation than normal isolates
599 (Kobayashi et al., 2015). In the Gobi Desert, dust events increase the diversity of
600 airborne microbial communities; after dust events, spore-forming bacteria, such as
601 *Bacillus*, increase in their relative abundances (Maki et al., 2016). Accordingly, in the
602 atmosphere, selected Bacilli members associated with dust particles would be
603 transported over long distances.

604 The Bacilli sequences showed different vertical variations between the two dust
605 events on March 19, 2013 and March 20, 2015. On March 19, 2013 (13H319-m), the
606 relative abundances of Bacilli sequences decreased dynamically from 3,000 m to 1,200
607 m, while unstable atmospheric layers on March 20, 2015 most likely mixed the
608 long-range transported bacteria with the regional bacteria over the Noto Peninsula. A
609 previous investigation also demonstrated the vertical mixture of airborne bacteria over
610 Suzu in the Noto Peninsula (Maki et al., 2010).

611 Actinobacteria sequences decreased in relative abundance between the 23rd and
612 29th of March 2014 corresponding with changes in the air mass trajectory roots from
613 north Asian regions, such as eastern Siberia and Japan (Fig. 7). Furthermore,
614 Actinobacteria sequences appeared in the samples collected from air masses that were
615 transported throughout the Korean Peninsula on March 19, 2013; April 28, 2013; and
616 March 20, 2015. Actinobacteria members are frequently dominant in terrestrial
617 environments but seldom survive in the atmosphere for a long time, because they cannot
618 form spores (Puspitasari et al., 2015). However, the family Micrococcaceae in
619 Actinobacteria was primarily detected from anthropogenic particles collected in Beijing,
620 China (Cao et al., 2014). Over anthropogenic source regions for Asian continents,

621 anthropogenic particles occupy more than 90 % of dust particles and originate from
622 soils disturbed by human activities in cropland, pastureland, and urbanized regions
623 (Huang et al., 2015a; Guan et al., 2016). Air masses transported from the continental
624 coasts are expected to include a relatively high abundance of Actinobacteria members
625 associated with anthropogenic particles.

626 Natural dust particles from Asian desert areas (Taklimkan and Gobi Deserts) are
627 transported in the free troposphere (Iwasaka et al., 1988) and vertically mixed with
628 anthropogenic particles during the transportation processes (Huang et al., 2015a). In
629 some cases, short-range transport of air masses would carry only anthropogenic
630 particles to Japan, because the anthropogenic particles are often dominant in Asian
631 continental coasts (Huang et al., 2015a). Actinobacteria members may have been
632 transported with anthropogenic particles from continental coasts.

633

634 *4.5 Dominant bacterial populations in the air masses originated from marine* 635 *environments and Japanese islands*

636 Proteobacteria sequences increased in their relative abundances at high altitudes
637 during non-dust sampling dates (13H428-u, 13H428-m, 14H328-u, 14H328-m, and
638 March 2014 series), when air mass origins at 1,200 m changed from the Korean
639 Peninsula to Japan (Fig. 7). Proteobacteria members were the dominate species in the
640 atmosphere over mountains (Bowers et al., 2012; Vaitilingom et al., 2012; Temkiv et al.,
641 2012), in the air samples collected on a tower (Fahlgren et al., 2010), and from the
642 troposphere (DeLeon-Rodriguez et al., 2013; Kourtev et al., 2011). In the phylum
643 proteobacteria, the families Phyllobacteriaceae, Methylobacteriaceae, and

644 Xanthomonadaceae were predominately detected from the non-dust samples and are
645 associated with plant bodies or surfaces (Mantelin et al., 2006; Fürnkranz et al., 2008;
646 Khan and Doty, 2009; Fierer and Lennon, 2011). The Betaproteobacteria sequences in
647 the non-dust samples mainly contained the Oxalobacteraceae and Comamonadaceae
648 families, which are commonly dominate in freshwater environments (Nold and Zwart,
649 1998) as well as on plant leaves (Redford et al., 2010). In addition, the class
650 Alphaproteobacteria in the non-dust samples also included marine bacterial sequences
651 belonging to the family Sphingomonadaceae (Cavicchioli et al., 2003). Bacterial
652 populations originating from marine areas are prevalent in cloud droplets (Amato et al.,
653 2007), in air samples collected from the seashores of Europe (Polymenakou et al., 2008),
654 in storming troposphere (DeLeon-Rodriguez et al., 2013), and at high altitudes in
655 Japanese regions (Maki et al., 2014), suggesting that the marine environments represent
656 a major source of bacteria in clouds. The air masses suspended over the Sea of Japan or
657 Japanese islands during non-dust events (the March 2014 series) could include a high
658 relative abundance of airborne bacteria, which were transported from the surface-level
659 air over the marine environments and the regional phyllosphere.

660

661 *4.6. Bacterial populations commonly detected during dust events and the non-dust* 662 *events*

663 Sequences originating from Synechococcaceae (in the class Cyanobacteria)
664 randomly appeared in the MiSeq sequencing databases results obtained from air samples,
665 regardless of dust event occurrences. *Synechococcus* species in the family
666 Synechococcaceae can eliminate excess peroxide from photosynthesis to resist UV

667 radiation and oxygenic stress (Latifi et al., 2009), suggesting that these bacteria resist
668 environmental stressors in the atmosphere. In a previous study, the air samples
669 transported from marine environments to Japan predominately contained *Synechococcus*
670 species (Maki et al., 2014), which were dominant marine bacteria in the Sea of Japan
671 and the East China Sea (Choi and Noh, 2009). The cloud water at approximately 3,000
672 m above ground level was also dominated by Cyanobacteria populations, indicating
673 their atmospheric transport (Kourtev et al., 2011). In addition to Alphaproteobacteria,
674 marine cyanobacterial cells can be transported from seawater to the atmosphere, thereby
675 contributing to the airborne bacterial variations over the Noto Peninsula. Marine
676 bioaerosols originated from cyanobacteria and gram-negative bacteria (including
677 Alphaproteobacteria) are reported to contribute the increase of endotoxin levels in
678 coastal areas influencing human health by inflammation and allergic reaction
679 (Lang-Yona et al., 2014).

680 Bacteroidetes sequences were detected in some air samples collected during Asian
681 dust and non-dust events. Members of the phylum Bacteroidetes, which were composed
682 of the families Cytophagaceae, associate with organic particles in terrestrial and aquatic
683 environments (Turnbaugh et al., 2011; Newton et al., 2011). Furthermore, these
684 bacterial populations dominate the atmosphere and sand of desert areas, where plant
685 bodies and animal feces are sparsely present (Maki et al., 2016). These bacterial groups
686 possibly originated from organic-rich microenvironments in several areas, such as desert
687 and marine areas.

688

689 **5. Conclusion**

690 Air samples including airborne bacteria were sequentially collected at high
691 altitudes over the Noto Peninsula during dust events and non-dust events. The sampled
692 air masses could be categorized based on sample types with (dust samples) and without
693 (non-dust samples) dust event influences. Bacterial communities in the air samples
694 displayed different compositions between dust events and non-dust events. The dust
695 samples were dominated by terrestrial bacteria, such as Bacilli, which are thought to
696 originate from the central desert regions of Asia, and the bacterial compositions were
697 similar between the dust samples. In contrast, the air masses of non-dust samples came
698 from several areas, including northern Asia, continental coasts, marine areas, and Japan
699 regional areas, showing different variations in bacterial compositions between the
700 sampling dates. Some scientists have attempted to apply airborne bacterial composition
701 as tracers of air mass sources at ground level (Bowers et al., 2011; Mazar et al., 2016).
702 In this study, the terrestrial bacteria, such as Bacilli and Actinobacteria members (Bottos
703 et al., 2014), were dominant populations in the air samples transported from Asian
704 continental areas. The air samples when the air mass was suspended around Japanese
705 islands, mainly included the members of the classes Alpha (Phyllobacteriaceae and
706 Methylobacteriaceae), Gamma, and Betaproteobacteria, which are commonly
707 dominated in phyllosphere (Redford et al., 2010; Fierer and Lennon, 2011) or
708 freshwater environments (Nold and Zwart, 1998). The atmospheric aerosols transported
709 via marine areas include a high relative abundances of marine bacteria belonging to
710 classes Cyanobacteria (Choi and Noh, 2009) and Alphaproteobacteria
711 (Sphingomonadaceae) (Cavicchioli et al., 2003). This study suggested that bacterial
712 compositions in the atmosphere can be used as air mass tracers, which could identify the

713 levels of mixed air masses transported from different sources.

714 However, one limitation of our investigation is that the number of samples
715 analyzed was not sufficient to cover entire changes in airborne bacteria at high altitudes
716 over the Noto Peninsula. Although the airborne bacterial composition during non-dust
717 periods was found to change dynamically, only a few types of variation were followed
718 in this investigation. In the future, greater numbers of samples, which are sequentially
719 collected at high altitudes using this sampling method, will need to be originated to
720 more accurately evaluate bioaerosol tracers. Since helicopter sampling procedures
721 require sophisticated techniques and are expensive, the sample numbers at high altitudes
722 are difficult to increase. Air sampling at high altitudes should be combined with
723 sequential ground-air sampling to advance the understanding of the influence of
724 westerly winds on airborne bacterial dynamics in downwind areas. Metagenomic
725 analyses and microbial culture experiments would also provide valuable information
726 about airborne microbial functions relating to ice-nucleation activities, chemical
727 metabolism, and pathogenic abilities.

728

729 **Acknowledgments**

730 We are thankful for the advice given by Dr. Richard C. Flagan of California Institute
731 of Technology and the sampling support from Dr. Atsushi Matsukia and Dr. Makiko
732 Kakikawa of Kanazawa University. Trajectories were produced by the NOAA Air
733 Resources Laboratory (ARL), which provided the HYSPLIT transport and dispersion
734 model and/or READY website (<http://www.ready.noaa.gov>). Members of Fasmac Co.,
735 Ltd. helped with the MiSeq sequencing analyses. This research was funded by the

736 Grant-in-Aid for Scientific Research (B) (No. 26304003) and (C) (No. 26340049). The
737 Bilateral Joint Research Projects from the Japan Society for the Promotion of Science
738 also supported this work, as did the Strategic International Collaborative Research
739 Program (SICORP: 7201006051) and Strategic Young Researcher Overseas Visits
740 Program for Accelerating Brain Circulation (No. G2702). This study was supported by
741 the Joint Research Program of Arid Land Research Center, Tottori University (No.
742 28C2015).

743

744 **Competing Interests**

745 The authors declare that they have no conflict of interest.

746

747 **References**

748 Amato, P., Parazols, M., Sancelme, M., Mailhot, G., Laj, P., and Delort, A.M.: An
749 important oceanic source of micro-organisms for cloud water at the Puy de Dôme
750 (France), *Atmos. Environ.*, 41, 8253–8263, 2007.

751 Atkinson, J.D., Murray, B.J., Woodhouse, M.T., Whale, T.F., Baustian, K.J., Carslaw,
752 K.S., Dobbie, S., O’Sullivan, D., Malkin, T.L.: The importance of feldspar for ice
753 nucleation by mineral dust in mixed-phase clouds, *Nature*, 498, 355–358, 2013.

754 Bottos, E.M., Woo, A.C., Zawar-Reza, P., Pointing, S.B., and Cary, S.C.: Airborne
755 Bacterial populations above desert soils of the McMurdo Dry Valleys, Antarctica,
756 *Microb. Ecol.*, 67, 120–128, 2014.

757 Bowers, R.M., McLetchie, S., Knight, R., and Fierer, N.: Spatial variability in airborne
758 bacterial communities across land-use types and their relationship to the bacterial

759 communities of potential source environments, *ISME J.*, 5, 601–612, 2011.

760 Bowers, R.M., McCubbin, I.B., Hallar, A.G., and Fierer, N.: Seasonal variability in
761 airborne bacterial communities at a high-elevation site, *Atmos. Environ.*, 50, 41–49,
762 2012.

763 Brodie, E.L., DeSantis, T.Z., Parker, J.P.M., Zubietta, I.X., Piceno, Y.M., Andersen,
764 G.L.: Urban aerosols harbor diverse and dynamic bacterial populations, *Proc. Natl.*
765 *Acad. Sci. U.S.A.*, 104, 299–304, 2007.

766 Brown, J.K.M., and Hovmøller, M.S.: Aerial dispersal of pathogens on the global and
767 continental scales and its impact on plant disease, *Science*, 297, 537–541, 2002.

768 Cao, C., Jiang, W., Wang, B., Fang, J., Lang, J., Tian, G., Jiang, J., and Zhu, T.F.:
769 Inhalable microorganisms in Beijing’s PM2.5 and PM10 pollutants during a severe
770 smog event, *Environ. Sci. Technol.*, 48, 1499–1507, 2014.

771 Caporaso, J.G., Kuczynski, J., Stombaugh, J., Bittinger, K., Bushman, F.D., Costello,
772 E.K., Fierer, N., Peña, A.G., Goodrich, J.K., Gordon, J.I., Huttley, G.A., Kelley,
773 S.T., Knights, D., Koenig, J.E., Ley, R.E., Lozupone, C.A., McDonald, D.,
774 Muegge, B.D., Pirrung, M., Reeder, J., Sevinsky, JR., Turnbaugh, P.J., Walters,
775 W.A., Widmann, J., Yatsunenko, T., Zaneveld, J., and Knight, R.: QIIME allows
776 analysis of high-throughput community sequencing data, *Nature methods*, 7,
777 335–336, 2010.

778 Caporaso, J.G., Lauber, C.L., Walters, W.A., Berg-Lyons, D., Lozupone, C.A.,
779 Turnbaugh, P.J., Fierer, N., and Knight, R.: Global patterns of 16S rRNA diversity
780 at a depth of millions of sequences per sample, *Proc. Natl. Acad. Sci.*, 108,
781 4516–4522, 2011.

782 Cavicchioli, R., Ostrowski, M., Fegatella, F., Goodchild, A., and Guixa-Boixereu, N.:
783 Life under nutrient limitation in oligotrophic marine environments: an
784 eco/physiological perspective of *Sphingopyxis alaskensis* (formerly *Sphingomonas*
785 *alaskensis*), *Microb. Ecol.*, 45, 203–217, 2003.

786 Choi, D.H., and Noh, J.H.: Phylogenetic diversity of *Synechococcus* strains isolated
787 from the East China Sea and the East Sea, *FEMS Microbiol. Ecol.*, 69, 439–448,
788 2009.

789 Chung, Y.S., and Kim, H.S.: Observations of massive-air pollution transport and
790 associated air quality in the Yellow Sea region, *Air Qual. Atmos. Health*, 1, 69–70,
791 2008.

792 Creamean, J. M., Suski, K. J., Rosenfeld, D., Cazorla, A., DeMott, P. J., Sullivan, R.C.,
793 White, A.B., Ralph, F.M., Minnis, P., Comstock, J.M., Tomlinson, J.M.: Dust and
794 biological aerosols from the Sahara and Asia influence precipitation in the western
795 U.S., *Science*, 339, 1572–1578, 2013.

796 DeLeon-Rodriguez, N., Latham, T.L., Rodriguez-R, L.M., Barazesh, J.M., Anderson,
797 B.E., Beyersdorf, A.J, Ziemba, L.D., Bergin, M., Nenes, A., and Konstantinidis,
798 K.T.: Microbiome of the upper troposphere: Species composition and prevalence,
799 effects of tropical storms, and atmospheric implications, *Proc. Natl. Acad. Sci.*
800 *USA*, 110, 2575–2580, 2013.

801 Delort, A.M., Vařtilingom, M., Amato, P., Sancelme, M., Parazols, M., Mailhot, G., Laj,
802 P., and Deguillaume, L.: A short overview of the microbial population in clouds:
803 Potential roles in atmospheric chemistry and nucleation processes, *Atmos. Res.*, 98,
804 249–260, 2010.

805 Edgar, R.C.: UPARSE: highly accurate OTU sequences from microbial amplicon reads,
806 Nature methods, 10, 996–998, 2013.

807 Fahlgren, C., Hagström, Å., Nilsson, D., and Zweifel, U.L.: Annual variations in the
808 diversity, viability, and origin of airborne bacteria, Appl. Environ. Microbiol., 76,
809 3015–3025, 2010.

810 Fierer, N., and Lennon, J.T.: The generation and maintenance of diversity in microbial
811 communities, American J. Botany, 98, 439–448, 2011.

812 Fu, P., Zhuang, G., Sun, Y., Wang, Q., Chen, J., Ren, L. Yang, F., Wang, Z., Pan, X., Li,
813 X., Kawamura, K.: Molecular markers of biomass burning, fungal spores and
814 biogenic SOA in the Taklimakan desert aerosols, Atmos. Environ., 130, 64-73,
815 2016.

816 Fürnkranz, M., Wanek, W., Richter, A., Abell, G., Rasche, F., and Sessitsch, A.:
817 Nitrogen fixation by phyllosphere bacteria associated with higher plants and their
818 colonizing epiphytes of a tropical lowland rainforest of Costa Rica, ISME J., 2 5,
819 561–570, 2008.

820 Gorbushina, A.A., Kort, R., Schulte, A., Lazarus, D., Schnetger, B., Brumsack, H.J.,
821 Broughton, W.J., and Favet, J.: Life in Darwin's dust: intercontinental transport and
822 survival of microbes in the nineteenth century, Environ. Microbiol., 9, 2911–2922,
823 2007.

824 Griffin, D.W.: Atmospheric movement of microorganisms in clouds of desert dust and
825 implications for human health, Clin. Microbiol. Rev., 20, 459–477, 2007.

826 Guan, X., Huang, J., Zhang, Y., Xie, Y., and Liu, J.: The relationship between
827 anthropogenic dust and population over global semi-arid regions, Atmos. Chem.

828 Phys., 16, 5159-5169, 2016.

829 Hallet, J., Mossop, S.C.: Production of secondary ice particles during the riming process,
830 Nature, 249, 26–28, 1974.

831 Hara, K., and Zhang, D.: Bacterial abundance and viability in long-range transported
832 dust, Atmos. Environ., 47, 20–25, 2012.

833 Hara, K., Maki, T., Kakikawa, M., Kobayashi, F., and Matsuki, A.: Effects of different
834 temperature treatments on biological ice, Atmos. Environ., 140, 415-419, 2016a.

835 Hara, K., Maki, T., Kobayashi, F., Kakikawa, M., Wada, M., and Matsuki, A.:
836 Variations of ice nuclei concentration induced by rain and snowfall within a local
837 forested site in Japan, Atmos. Environ., 127, 1–5, 2016b.

838 Hoose, C., Möhler, O.: Heterogeneous ice nucleation on atmospheric aerosols: a review
839 of results from laboratory experiments, Atmos. Chem. Phys., 12, 9817–9854. 2012.

840 Hua, N.P., Kobayashi, F., Iwasaka, Y., Shi, G.Y., and Naganuma, T.: Detailed
841 identification of desert-originated bacteria carried by Asian dust storms to Japan,
842 Aerobiologia, 23, 291–298, 2007.

843 Huang, J.P., Liu, J.J., Chen, B., and Nasiri, S.L.: Detection of anthropogenic dust using
844 CALIPSO lidar measurements, Atmos. Chem. Phys., 15, 11653-11665, 2015a.

845 Huang, Z., Huang, J., Hayasaka, T., Wang, S., Zhou, T., and Jin, H.: Short-cut transport
846 path for Asian dust directly to the Arctic: a case study, Environ. Res. Lett., 10,
847 114018, 2015b.

848 Ichinose, T., Nishikawa, M., Takano, H., Sera, N., Sadakane, K., Mori, I., Yanagisawa,
849 R., Oda, T., Tamura, H., Hiyoshi, K., Quan, H., Tomura, S., and Shibamoto, T.:
850 Pulmonary toxicity induced by intratracheal instillation of Asian yellow dust

851 (Kosa) in mice, *Regul. Toxicol. Pharm.*, 20, 48-56, 2005.

852 Iwasaka, Y., Shi, G.Y., Yamada, M., Kobayashi, F., Kakikawa, M., Maki, T., Chen, B.,
853 Tobo, Y., and Hong, C.: Mixture of Kosa (Asian dust) and bioaerosols detected in
854 the atmosphere over the Kosa particles source regions with balloon-borne
855 measurements: possibility of long-range transport, *Air. Qual. Atmos. Health.*, 2,
856 29–38, 2009.

857 Iwasaka, Y., Yamato, M., Imasu, R., and Ono, A.: The transport of Asia dust (KOSA)
858 particles; importance of weak KOSA events on the geochemical cycle of soil
859 particles, *Tellus*, 40B, 494–503, 1988.

860 Jaenicke, R.: Abundance of cellular material and proteins in the atmosphere, *Science*,
861 308, 73, 2005.

862 Jeon, E.M., Kim, H.J., Jung, K., Kim, J.H., Kim, M.Y., Kim, Y.P., and Ka, J.O.: Impact
863 of Asian dust events on airborne bacterial community assessed by molecular
864 analyses, *Atmos. Environ.*, 45, 4313–4321, 2011.

865 Joly, M., Attard, E., Sancelme, M., Deguillaume, L., Guilbaud, C., Morris, C.E. Amato,
866 P., and Delort, A.M.: Ice nucleation activity of bacteria isolated from cloud water,
867 *Atmos. Environ.*, 70, 392–400, 2013.

868 Khan, Z., and Doty, S.L.: Characterization of bacterial endophytes of sweet potato
869 plants, *Plant Soil*, 322, 197–207, 2009.

870 Kobayashi, F., Iwata, K., Maki, T., Kakikawa, M., Higashi, T., Yamada, M., Ichinose, T.,
871 and Iwasaka, Y.: Evaluation of the toxicity of a Kosa (Asian duststorm) event from
872 view of food poisoning: observation of Kosa cloud behavior and real-time PCR
873 analyses of Kosa bioaerosols during May 2011 in Kanazawa, Japan, *Air Qual.*

874 Atmos. Health, 9, 3–14, 2015.

875 Kourtev, P.S., Hill, K.A., Shepson, P.B., and Konopka A.: Atmospheric cloud water
876 contains a diverse bacterial community, Atmos. Environ., 45, 5399–5405, 2011.

877 Lang-Yona, N., Lehahn, Y., Herut, B., Burshtein, N., and Rudich, Y.: Marine aerosol as
878 a possible source for endotoxins in coastal areas, Sci. Total Environ., 499, 311–318,
879 2014.

880 Latifi, A., Ruiz, M., and Zhang, C.C.: Oxidative stress in cyanobacteria, FEMS
881 Microbiol. Rev., 33, 258–278, 2009.

882 Liu, B., Ichinose, T., He, M., Kobayashi, N., Maki, T., Yoshida, S., Yoshida, Y.,
883 Arashidani, K., Nishikawa, M., Takano, H., Sun, G., and Shibamoto, T.: Lung
884 inflammation by fungus, *Bjerkandera adusta* isolated from Asian sand dust (ASD)
885 aerosol and enhancement of ovalbumin -induced lung eosinophilia by ASD and the
886 fungus in mice, Allergy Asthma Clin. Immunol., 10, 10, 2014.

887 Maki, T., Kurosaki, Y., Onishi, K., Lee, K.C., Pointing, S.B., Jugder, D., Yamanaka, N.,
888 Hasegawa, H., and Shinoda, M.: Variations in the structure of airborne bacterial
889 communities in Tsogt-Ovoo of Gobi Desert area during dust events, Air Qual.
890 Atmos. Health., 2016. DOI: 10.1007/s11869-016-0430-3

891 Maki, T., Susuki, S., Kobayashi, F., Kakikawa, M., Tobo, Y., Yamada, M., Higashi, T.,
892 Matsuki, A., Hong, C., Hasegawa, H., and Iwasaka, Y.: Phylogenetic analysis of
893 atmospheric halotolerant bacterial communities at high altitude in an Asian dust
894 (KOSA) arrival region, Suzu City, Sci. Total Environ., 408, 4556–4562, 2010.

895 Maki, T., Hara, K., Kobayashi, F., Kurosaki, Y., Kakikawa, M., Matsuki, A., Bin, C., Shi,
896 G., Hasegawa, H., and Iwasaka, Y.: Vertical distribution of airborne bacterial

897 communities in an Asian-dust downwind area, Noto Peninsula, Atmos. Environ.,
898 119, 282–293, 2015.

899 Maki, T., Kakikawa, M., Kobayashi, F., Yamada, M., Matsuki, A., Hasegawa, H., and
900 Iwasaka, Y.: Assessment of composition and origin of airborne bacteria in the free
901 troposphere over Japan, Atmos. Environ., 74, 73–82, 2013.

902 Maki, T., Susuki, S., Kobayashi, F., Kakikawa, M., Yamada, M., Higashi, T., Chen, B.,
903 Shi, G., Hong, C., Tobo, Y., Hasegawa, H., Ueda, K., and Iwasaka, Y.:
904 Phylogenetic diversity and vertical distribution of a halobacterial community in the
905 atmosphere of an Asian dust (KOSA) source region, Dunhuang City, Air. Qual.
906 Atmos. Health, 1, 81–89, 2008.

907 Maki, T., Puspitasari, F., Hara, K., Yamada, M., Kobayashi, F., Hasegawa, H., and
908 Iwasaka, Y.: Variations in the structure of airborne bacterial communities in a
909 downwind area during an Asian dust (Kosa) event, Sci. Total Environ., 488–489,
910 75–84, 2014.

911 Mantelin, S., Fischer-Le Saux, M., Zakhia, F., Béna, G., Bonneau, S., Jeder, H., Lajudie,
912 P., and Cleyet-Marel, J.C.: Emended description of the genus *Phyllobacterium* and
913 description of four novel species associated with plant roots: *Phyllobacterium*
914 *bourgognense* sp. nov., *Phyllobacterium ifriqiyense* sp. nov., *Phyllobacterium*
915 *leguminum* sp. nov. and *Phyllobacterium brassicacearum* sp. nov., Int. J Syst. Evol.
916 Microbiol., 56, 827–839, 2006.

917 Matulova, M., Husarova, S., Capek, P., Sancelme, M., and Delort, A.M.:
918 Biotransformation of various saccharides and production of exopolymeric
919 substances by cloud-borne *Bacillus* sp. 3B6, Environ. Sci. Technol., 48,

920 14238–14247, 2014.

921 Mazar, Y., Cytryn, E., Erel, Y., and Rudich, Y.: Effect of dust storms on the atmospheric
922 microbiome in the Eastern Mediterranean, *Environ. Sci. Technol.*, 50, 4194–4202,
923 2016.

924 McDonald, D., Price, M.N., Goodrich, J., Nawrocki, E.P., DeSantis, T.Z., Probst, A.,
925 Andersen, G.L., Knight, R., and Hugenholtz, P.: An improved Greengenes
926 taxonomy with explicit ranks for ecological and evolutionary analyses of bacteria
927 and archaea, *ISME J.*, 6, 610–618, 2012.

928 Möhler, O., DeMott, P.J., Vali, G., and Levin, Z.: Microbiology and atmospheric
929 processes: the role of biological particles in cloud physics, *Biogeosciences*, 4,
930 1059–1071, 2007.

931 Morris, C.E., Georgakopoulos, D.G., Sands, D.C.: Ice nucleation active bacteria and
932 their potential role in precipitation, *J. Phy. IV France*, 121, 87–103. 2004.

933 Morris, C.E., Sands, D.C., Vinatzer, B.A., Glaux, C., Guilbaud, C., Buffière, A., Yan, S.,
934 Dominguez, H., and Thompson, B.M.: The life history of the plant pathogen
935 *Pseudomonas syringae* is linked to the water cycle, *ISME J.*, 2, 321–334, 2008.

936 Morris, C.E., Sands, D.C., Bardin, M., Jaenicke, R., Vogel, B., Leyronas, C., Ariya, P.A.,
937 Psenner, R.: Microbiology and atmospheric processes: research challenges
938 concerning the impact of airborne micro-organisms on the atmosphere and climate,
939 *Biogeoscience*, 8, 17–25. 2011.

940 Mortazavi, R., Attiya, S., and Ariya, P.A.: Arctic microbial and next-generation
941 sequencing approach for bacteria in snow and frost flowers: selected identification,
942 abundance and freezing nucleation, *Atmos. Chem. Phys.*, 15, 6183–6204, 2015.

943 Mostajir, B., Dolan, J.R., and Rassoulzadegan, F.: A simple method for the
944 quantification of a class of labile marine pico- and nano-sized detritus: DAPI
945 Yellow Particles (DYP), *Aquat. Microb. Ecol.*, 9, 259–266, 1995.

946 Murray, B.J., O’Sullivan, D., Atkinson, J.D., Webb, M.E.: Ice nucleation by particles
947 immersed in supercooled cloud droplets, *Chem. Soc. Rev.*, 41, 6519–6554. 2012.

948 Newton, R.J., Jones, S.E., Eiler, A., McMahon, K.D., and Bertilsson, S.: A guide to the
949 natural history of freshwater lake bacteria, *Microbiol. Mol. Biol. Rev.*, 75, 14–49,
950 2011.

951 Nicholson, W.L., Munakata, N., Horneck, G., Melosh, H.J., and Setlow, P.: Resistance
952 of *Bacillus* endospores to extreme terrestrial and extraterrestrial environments,
953 *Microbiol. Mol. Biol. Rev.*, 64, 548-572, 2000.

954 Nold, S.C., and Zwart, G.: Patterns and governing forces in aquatic microbial
955 communities, *Aquat. Ecol.*, 32:17–35, 1998.

956 Pointing, S.B., and Belnap, J.: Disturbance to desert soil ecosystems contributes to
957 dust-mediated impacts at regional scales, *Biodivers. Conserv.*, 24, 1659–1667,
958 2014.

959 Polymenakou, P.N., Mandalakis, M., Stephanou, E.G., and Tselepidis, A.: Particle size
960 distribution of airborne microorganisms and pathogens during an intense African
961 dust event in the Eastern Mediterranean, *Environ. Health Perspect.*, 116, 292–296,
962 2008.

963 Pratt, K.A., DeMott, P.J., French, J.R., Wang, Z., Westphal, D.L., Heymsfield, A.J.,
964 Twohy, C.H., Prenni, A.J., and Prather, K.A.: In situ detection of biological
965 particles in cloud ice-crystals, *Nature Geoscience*, 2, 398–401, 2009.

966 Puspitasari, F, Maki, T, Shi, G, Bin, C, Kobayashi, F, Hasegawa, H., and Iwasaka, Y.:
967 Phylogenetic analysis of bacterial species compositions in sand dunes and dust
968 aerosol in an Asian dust source area, the Taklimakan Desert, *Air Qual. Atmos.*
969 *Health.*, 9: 631–644, 2015.

970 Redford, A.J., Bowers, R.M., Knight, R., Linhart, Y., and Fierer, N.: The ecology of the
971 phyllosphere: geographic and phylogenetic variability in the distribution of
972 bacteria on tree leaves, *Environ. Microbiol.*, 12: 2885–2893, 2010.

973 Rodó, X., Ballester, J., Cayan, D., Melish, M.E., Nakamura, Y., Uehara, R., and Burns,
974 J.C.: Association of Kawasaki disease with tropospheric wind patterns, *Scientific*
975 *Reports* 1, 152, 2011.

976 Russell, W.C., Newman, C., and Williamson, D.H.: A simple cytochemical technique for
977 demonstration of DNA in cells infected with mycoplasmas and viruses, *Nature*,
978 253, 461–462, 1974.

979 Schloss, P.D., Westcott, S.L., Ryabin, T., Hall, J.R., Hartmann, M., Hollister, E.B.,
980 Lesniewski, R.A., Oakley, B.B., Parks, D.H., Robinson, C.J., Sahl, J.W., Stres,
981 B., Thallinger, G.G., Horn, D.J.V., and Weber, C.F.: Introducing mothur:
982 open-source, platform-independent, community-supported software for
983 describing and comparing microbial communities, *Appl. Environ. Microbiol.*,
984 75:7537–7541, 2009.

985 Sheridan, P.P., Miteva, V.I., and Brenchley, J.E.: Phylogenetic analysis of anaerobic
986 psychrophilic enrichment cultures obtained from a Greenland glacier ice core,
987 *Appl. Environl. Microbiol.*, 69, 2153–2160, 2003.

988 Smith, D.J., Timonen, H.J., Jaffe, D.A., Griffin, D.W., Birmele, M.N., Warda, P.P.D.,

989 and Roberts, M.S.: Intercontinental dispersal of bacteria and archaea by
990 transpacific winds, *Appl. Environl. Microbiol.*, 79, 1134–1139, 2013.

991 Sugimoto, N., Huang, Z., Nishizawa, T., Matsui, I., and Tatarov, B.: Fluorescence from
992 atmospheric aerosols observed with a multi-channel lidar spectrometer, *Optics*
993 *Express*, 20, 20800–20807, 2012.

994 Tanaka, D., Tokuyama, Y., Terada, Y., Kunimochi, K., Mizumaki, C., Tamura, S.,
995 Wakabayashi, M., Aoki, K., Shimada, W., Tanaka, H., and Nakamura, S.: Bacterial
996 communities in Asian dust-containing snow layers on Mt. Tateyama, Japan, *Bull.*
997 *Glaciological. Res.*, 29, 31–39, 2011.

998 Temkiv, T.Š., Kai F., Bjarne, M.H., Niels, W.N., and Ulrich, G.K.: The microbial
999 diversity of a storm cloud as assessed by hailstones, *FEMS Microbial. Ecol.*, 81,
1000 684–695, 2012.

1001 Turnbaugh, P.J., Biomolecules, S.B.D., and Roscoff, F.: Environmental and gut
1002 bacteroidetes: the food connection, *Front Microbiol.*, 2, 93–111, 2011.

1003 Twohy, C.H., McMeeking, G.R., DeMott, P.J., McCluskey, C.S., Hill, T.C., Burrows,
1004 S.M., G.R. Kulkarni, M. Tanarhte, and D.N. Kafle, and Toohey, D.W.: Abundance
1005 of fluorescent biological aerosol particles at temperatures conducive to the
1006 formation of mixed-phase and cirrus clouds, *Atmos. Chem. Phys.*, 16, 8205–8225,
1007 2016.

1008 Vařtilingom, M., Attard, E., Gaiani, N., Sancelme, M., Deguillaume, L., Flossmann, A.I.,
1009 Amato, P., and Delort, A.M.: Long-term features of cloud microbiology at the puy
1010 de Dôme (France), *Atmos. Environ.*, 56, 88–100, 2012.

1011 Watanabe, K., Yachi, C., Nishibe, M., Michigami, S., Saito, Y., Eda, N., Yamazaki, N.,

1012 and Hirai, T.: Measurements of atmospheric hydroperoxides over a rural site in
1013 central Japan during summers using a helicopter, *Atmos. Environ.*, 146, 174–182,
1014 2016.

1015 Wang, Q., Garrity, G.M., Tiedje, J.M., and Cole, J.R.: Naive Bayesian classifier for
1016 rapid assignment of rRNA sequences into the new bacterial taxonomy, *Appl.*
1017 *Environ. Microbiol.*, 73, 5261–5267, 2007.

1018 Wei, K., Zou, Z., Zheng, Y., Li, J., Shen, F., Wu, C. Y., Hua, M., and Yao, M.: Ambient
1019 bioaerosol particle dynamics observed during haze and sunny days in Beijing,
1020 *Sci. Total Environ.*, 550, 751–759, 2016.

1021 Woo, A.C., Brar, M.S., Chan, Y., Lau, M.C., Leung, F.C., Scott, J.A., Vrijmoed L.P.,
1022 Zawar-Reza P., and Pointing S.B.: Temporal variation in airborne microbial
1023 populations and microbially-derived allergens in a tropical urban landscape, *Atmos.*
1024 *Environ.*, 74, 291-300, 2013.

1025

1026 **Figure Legends**

1027

1028 Fig. 1. Sampling location (a) and helicopter flight routes during the sampling periods on
1029 March 19, 2013, and April 28, 2013 (b); the 23rd, 24th, 25th, and 29th of March 2014
1030 (c); and the 16th, 17th, 20th, and 21st of March 2015 (d).

1031

1032 Fig. 2. LIDAR observation of the depolarization ratio in Toyama city as well as vertical
1033 changes in temperature, relative humidity, and potential temperature, and vertical
1034 distributions of concentrations of OPC-counted particles and DAPI-stained particles
1035 from the four sampling events on March 19, 2013 (a); April 28, 2013 (b); March 28,
1036 2014 (c); and March 20, 2015 (d). The red circles in the LIDAR images indicate that the
1037 sampling air included dust mineral particles (solid line) or that dust-event influences are
1038 absent at the altitudes on the sampling time (dotted line). OPC-counted particles were
1039 categorized according to diameter sizes of 0.3–0.5 μm (closed squares), 0.5–0.7 μm
1040 (closed triangles), 0.7–1.0 μm (closed circles), 1.0–2.0 μm (closed diamonds), 2.0–5.0
1041 μm (crosses), and $>5.0 \mu\text{m}$ (open circles). DAPI-stained particles were classified into
1042 microbial particles (blue bars), white particles (white bars), yellow fluorescent particles
1043 (yellow bars), and black carbon (gray bars).

1044

1045 Fig. 3. Trajectories 3 days ago of aerosols that arrived at 2,500 m (blue-type lines) and
1046 1,200 m (red-type lines) in Hakui, Japan, every hour for 5 h before the completion of
1047 sampling time at the four dates; March 19, 2013; April 28, 2013; March 28, 2014; and
1048 March 20, 2015.

1049

1050 Fig. 4. (a) LIDAR observation of the depolarization ratio in Toyama city and
1051 concentrations of OPC-counted particles and DAPI-stained particles during no-dust
1052 days from 0:00 UTC on March 23 to 0:00 UTC on March 30, 2014. The red circles with
1053 dotted lines in the LIDAR images indicate dust-event influences are absent at the
1054 altitudes on the sampling time. (b) OPC-counted particles were categorized according to
1055 diameter sizes of 0.3–0.5 μm (closed squares), 0.5–0.7 μm (closed triangles), 0.7–1.0
1056 μm (closed circles), 1.0–2.0 μm (closed diamonds), 2.0–5.0 μm (crosses), and >5.0 μm
1057 (open circles). DAPI-stained particles were classified into microbial particles (blue bars),
1058 white particles (white bars), yellow particles (yellow bars), and black particles (gray
1059 bars). (c) Trajectories 3 days ago of aerosols that arrived at 2,500 m (blue-type lines)
1060 and 1,200 m (red-type lines) in Hakui, Japan, every hour for 5 h before the completion
1061 of sampling time during sampling periods on the 23rd, 24th, 25th, 28th, and 29th of
1062 March 2014.

1063

1064 Fig. 5. (a) LIDAR observation of the depolarization ratio in Toyama city and
1065 concentrations of OPC-counted particles and DAPI-stained particles during dust event
1066 days from 0:00 UTC on March 16 to 0:00 UTC on March 23, 2015. The red circles with
1067 solid lines in the LIDAR images indicate that the sampling air included dust mineral
1068 particles. (b) OPC-counted particles were categorized based on diameter sizes of
1069 0.3–0.5 μm (closed squares), 0.5–0.7 μm (closed triangles), 0.7–1.0 μm (closed circles),
1070 1.0–2.0 μm (closed diamonds), 2.0–5.0 μm (crosses), and >5.0 μm (open circles).
1071 DAPI-stained particles were classified into microbial particles (blue bars), white

1072 particles (white bars), yellow particles (yellow bars), and black particles (gray bars). (c)
1073 Trajectories 3 days ago of aerosols that arrived at 2,500 m (blue-type lines) and 1,200 m
1074 (red-type lines) in Hakui, Japan, every hour for 5 h before the completion of sampling
1075 time during sampling periods on the 16th, 17th, 20th, and 21st of March 2015.

1076

1077 Fig. 6. Vertical variations in bacterial compositions at (a) the class level and (b) the
1078 family level of the partial sequences obtained in the MiSeq sequencing database (ca.
1079 400 bp) obtained from air samples collected at different altitudes over the Noto
1080 Peninsula at dust-event days (March 19, 2013; March 20, 2015) and non-dust-event
1081 days (March 19, 2013; March 20, 2015).

1082

1083 Fig. 7. Changes in bacterial compositions at (a) the class level and (b) the family level
1084 of the partial sequences obtained in the MiSeq sequencing database (ca. 400 bp) from
1085 air samples collected at altitudes of 1,200 m (except for the sample collected at 500 m
1086 on March 20, 2015) over the Noto Peninsula during dust-event days from the 16th to the
1087 23rd of March 2015 and during non-dust-event days from the 23rd to the 29th of March
1088 2014.

1089

1090 Fig. 8. Comparison of the bacterial compositions among all air samples collected over
1091 the Noto Peninsula. (a) Box plots of Chao 1 and Shannon analyses indicating the
1092 bacterial diversity observed in dust samples and non-dust samples. Species were binned
1093 at the 97 % sequence similarity level. (b) NMDS of the pairwise Bray-Curtis distance
1094 matrix displaying clustering by all the air samples. Red indicates the samples that were

1095 collected during dust-events and blue indicates those collected during non-dust-events
1096 as determined by meteorological data. Circle indicates that the sample contained dust
1097 particles as identified via microscopic observation, and triangle indicates that dust
1098 particles were absent from the sample. The confidence ellipses are based on a
1099 multivariate t-distribution, and represents the 95 % confidence interval of the
1100 occurrence of dust vs. non-dust events when the samples were collected.

Table 1 Sampling information during the sampling periods.

Sample name	Sampling date	Collection time (JST)	Total time (min)	Air volume	Sampling method	Sampling location ^{*1}	Free troposphere ^{*2}
13H319-u	19 March 2013	14:04 – 15:04	60	700 L	helicopter	2500m	FT
13H319-m		15:19 – 16:19	60	700 L	helicopter	1200m	ABL
13H319-l		14:25 – 15:25	60	700 L	building	10m	GL
13H428-u	28 April 2013	12:10 – 13:04	56	653 L	helicopter	2500m	FT
13H428-m		13:13 – 14:03	50	583 L	helicopter	1200m	ABL
13H428-l		12:03 – 13:03	60	700 L	building	10m	GL
14H328-u	28 March 2014	12:50 – 13:50	60	700 L	helicopter	3000m	FT
14H328-m		14:04 – 15:04	60	700 L	helicopter	1200m	ABL
14H328-l		13:00 – 14:00	60	700 L	building	10m	GL
15H320-u	20 March 2015	12:26 – 13:23	47	548 L	helicopter	2500m	FT
15H320-m		13:39 – 14:40	60	711 L	helicopter	500m	ABL
14H323-m	23 March 2014	10:45 – 11:02	17	11.1 L	helicopter	1200m	ABL
14H324-m	24 March 2014	9:09 – 9:30	21	13.7 L	helicopter	1200m	ABL
14H325-m	25 March 2014	9:31 – 9:50	29	18.9 L	helicopter	1200m	ABL
14H328-m	28 March 2014	14:04 – 15:04	60	700 L	helicopter	1200m	ABL
14H329-m	29 March 2014	9:06 – 9:24	15	9.75 L	helicopter	1200m	PT
15H316-m	16 March 2015	11:21 – 11:43	22	14.3 L	helicopter	1200m	FT
15H317-m	17 March 2015	11:04 – 11:31	27	17.6 L	helicopter	1200m	FT
15H320-u	20 March 2015	12:26 – 13:23	47	548 L	helicopter	2500m	FT
15H321-m	21 March 2015	15:35 – 15:55	20	13.0 L	helicopter	1200m	FT

*1 Height above the ground.

*2 Free troposphere: FT, Atmospheric boundary layer: ABL, Phase transiens: PT, GL: Ground level

Table 2. Researches targeting bacterial communities associated with Asian-dust events

Sampling area ^{*1}	Sample	Location	Altitudes (m)	Sampling place	Sampling method	Analytical method for microorganisms	Dominated bacteria ^{*2}			references
							1st	2nd	3rd	
Dust source area	Soil	Taklamakan Desert, China	0	Ground surface	soil sampling	clone library	Bacteroidetes (Sphingobacteriia)	Actinobacteria (Actinobacteria)	Proteobacteria (Alpha, Beta, Gamma)	Yamaguchi et al. 2012
Dust source area	Soil	Gobi Desert, China	0	Ground surface	soil sampling	clone library	Actinobacteria (Actinobacteria)	Proteobacteria (Beta)	Bacteroidetes (Sphingobacteriia)	Yamaguchi et al. 2012
Dust source area	Soil	Taklamakan Desert, China	0	Ground surface	soil sampling	pyrosequencing	Firmicutes (Bacilli)†	Actinobacteria	Proteobacteria (Gamma)	An et al. 2013
Dust source area	Soil	Gobi Desert, China	0	Ground surface	soil sampling	pyrosequencing	Firmicutes (Bacilli)†	Proteobacteria (Gamma)	Bacteroidetes	An et al. 2013
Dust source area	Soil	Taklamakan, China	0	Ground surface	soil samples	clone library	Actinobacteria (Actinobacteria)	Firmicutes (Bacilli)	Proteobacteria	Puspitasari et al. 2016
Dust source and deposition area	Soil	Loess plateau, China	0	Ground surface	soil sampling	clone library	Proteobacteria (Beta, Gamma)	Actinobacteria (Actinobacteria)	Bacteroidetes (Sphingobacteriia)	Yamaguchi et al. 2012
Dust source and deposition area	Soil	Loess plateau, China	0	Ground surface	soil sampling	PCR-DGEE	Proteobacteria	Bacteroidetes	Gemmatimonadetes	Kenzaki et al. 2010
Dust source area	Air	Tsogt-Ovoo, Mongolia	3	Ground surface	filtration	MISeq sequencing	Proteobacteria (Alpha)	Firmicutes (Bacilli)	Actinobacteria (Actinobacteria)	Maki et al. 2017
Dust source area	Air	Dunhuang, China	10	Top of building	filtration	clone library	Firmicutes (Bacilli)†	Proteobacteria	Bacteroidetes	Puspitasari et al. 2016
Dust source area	Air	Dunhuang, China	800	Balloon	filtration	PCR-DGEE	Firmicutes (Bacilli)†	-	-	Maki et al. 2008
Dust source area	Air	Dunhuang, China	800	Balloon	filtration	clone library	Proteobacteria (Gamma)	Firmicutes (Bacilli)	-	Kakikawa et al. 2009
Dust deposition area	Air	Noto peninsula, Japan	3000	Aircraft	filtration	clone library	Firmicutes (Bacilli)†	Bacteroidetes (Bacteroidia)	Proteobacteria (Gamma)	Maki et al. 2013
Dust deposition area	Air	Noto peninsula, Japan	3000	Aircraft	filtration	MISeq sequencing	Firmicutes (Bacilli)†	Actinobacteria (Actinobacteria)	Proteobacteria (Alpha&Beta)	Maki et al. 2015
Dust deposition area	Air	Mt. Bachelor Observatory, USA	2700	Mt. Bachelor	filtration	culture	Firmicutes (Bacilli)†	Actinobacteria (Actinobacteria)	Proteobacteria (Gamma)	Smith et al. 2012
Dust deposition area	Air	Mt. Bachelor Observatory, USA	2700	Mt. Bachelor	filtration	Microarray	Proteobacteria (Beta&Gamma)	Actinobacteria (Actinobacteria)	Firmicutes (Bacilli)†	Smith et al. 2013
Dust deposition area	Snow	Mt. Tateyama, Japan	2450	Mt. Tateyama	Snow sampling	PCR-DGEE	Firmicutes (Bacilli)†	Proteobacteria (Beta, Gamma)	Actinobacteria (Actinobacteria)	Tanaka et al. 2011
Dust deposition area	Snow	Mt. Tateyama, Japan	2450	Mt. Tateyama	Snow sampling	PCR-DGEE	Firmicutes (Bacilli)†	Proteobacteria (Beta)	Actinobacteria (Actinobacteria)	Maki et al. 2011
Dust deposition area	Air	Noto peninsula, Japan	1200	Helicopter	filtration	MISeq sequencing	Firmicutes (Bacilli)†	Proteobacteria (Alpha, Gamma)	Cyanobacteria	This study
Dust deposition area	Air	Suzu, Japan	1000	Balloon	filtration	MISeq sequencing	Firmicutes (Bacilli)†	Proteobacteria (Alpha)	Deinococcus-Thermus (Deinococci)	Maki et al. 2015
Dust deposition area	Air	Osaka, Japan	900	Air craft	filtration	clone library	Firmicutes (Bacilli)	Bacteroidetes (Sphingobacteriia)	Actinobacteria (Actinobacteria)	Yamaguchi et al. 2012
Dust deposition area	Air	Suzu, Japan	800	Balloon	filtration	clone library	Firmicutes (Bacilli)†	Bacteroidetes (Bacteroidia)	Proteobacteria (Gamma)	Maki et al. 2013
Dust deposition area	Air	Suzu, Japan	600	Balloon	filtration	PCR-DGEE	Firmicutes (Bacilli)†	-	-	Maki et al. 2010
Dust deposition area	Air	Seoul, South Korea	25	Top of building	liquid impiger	pyrosequencing	Actinobacteria (Actinobacteria)	Proteobacteria (Alpha, Gamma)	Firmicutes (Bacilli)†	Cha et al. 2017
Dust deposition area	Air	Osaka, Japan	20	Top of building	filtration	pyrosequencing	Actinobacteria (Actinobacteria)	Cyanobacteria	Acidobacteria (Acidobacteria)	Park et al. 2016
Dust deposition area	Air	Seoul, South Korea	17	Top of building	filtration	PCR-DGEE	Actinobacteria (Actinobacteria)	Firmicutes (Bacilli)†	Proteobacteria (Gamma)	Lee et al. 2011
Dust deposition area	Air	Beijing, China	15	Top of building	filtration	pyrosequencing	Firmicutes (Bacilli)	Proteobacteria (Gamma)	Bacteroidetes (Flavobacteriia)	Wei et al. 2016
Dust deposition area	Air	Beijing, China	10	Top of building	filtration	HiSeq sequencing	Actinobacteria (Actinobacteria)	Proteobacteria (Alpha, Beta, Gamma)	Chloroflexi (Thermomicrobia)	Cao et al. 2014
Dust deposition area	Air	Seoul, South Korea	10	Top of building	filtration	clone library	Firmicutes (Bacilli)†	Actinobacteria	Bacteroidetes	Jeon et al. 2011
Dust deposition area	Air	Suzu, Japan	10	Top of building	filtration	MISeq sequencing	Firmicutes (Bacilli)†	Deinococcus-Thermus (Deinococci)	Proteobacteria (Alpha)	Maki et al. 2015
Dust deposition area	Air	Goyang, South Korea	-	Top of building	filtration	pyrosequencing	Actinobacteria (Actinobacteria)	Proteobacteria (Gamma)	Firmicutes (Bacilli)†	Cha et al. 2016
Dust deposition area	Air	Kanazawa, Japan	10	Roof of building	filtration	MISeq sequencing	Firmicutes (Bacilli)†	Cyanobacteria	Proteobacteria (Alpha)	Maki et al. 2014
Dust deposition area	Air	Western Pacific Ocean	-	Ship board	filtration	pyrosequencing	Firmicutes (Bacilli)†	Proteobacteria (Beta, Gamma)	Cyanobacteria	Xia et al. 2015

*1 Dust source area: the areas providing dust mineral particles. Dust deposition area: the area where the dust mineral particles deposit

*2 The bacterial phyla in the orders of large abundance rates in each samples.

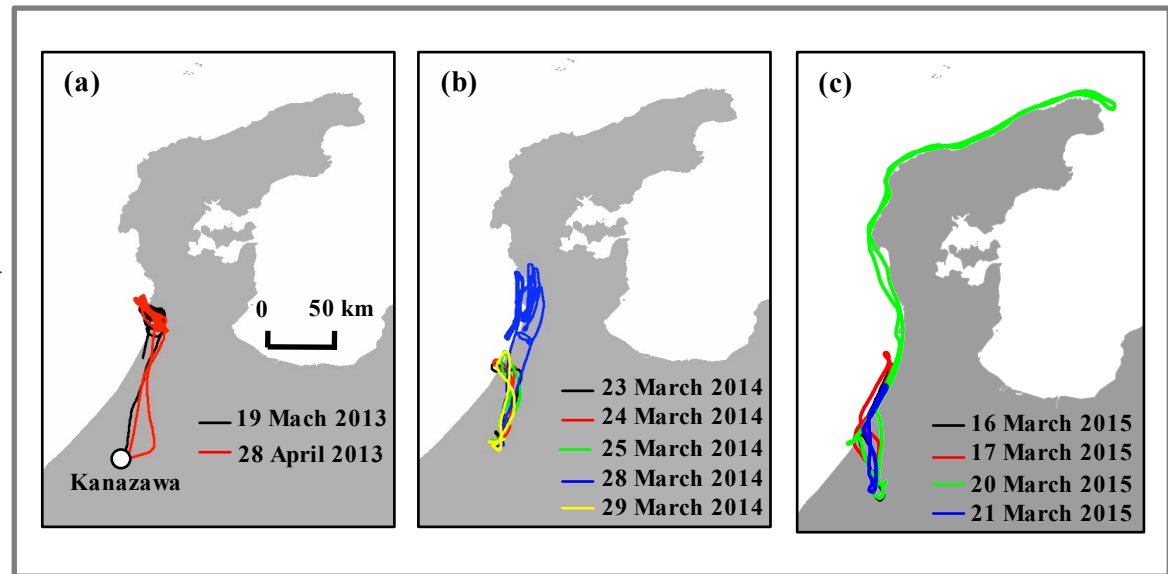
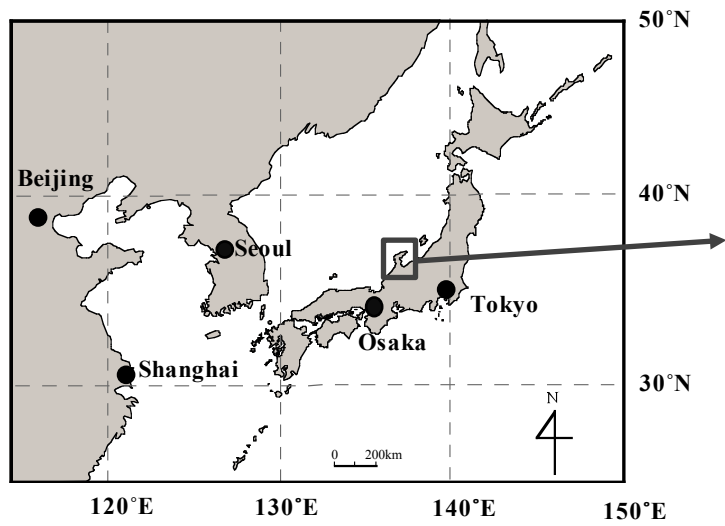


Fig. 1 T. Maki et al.

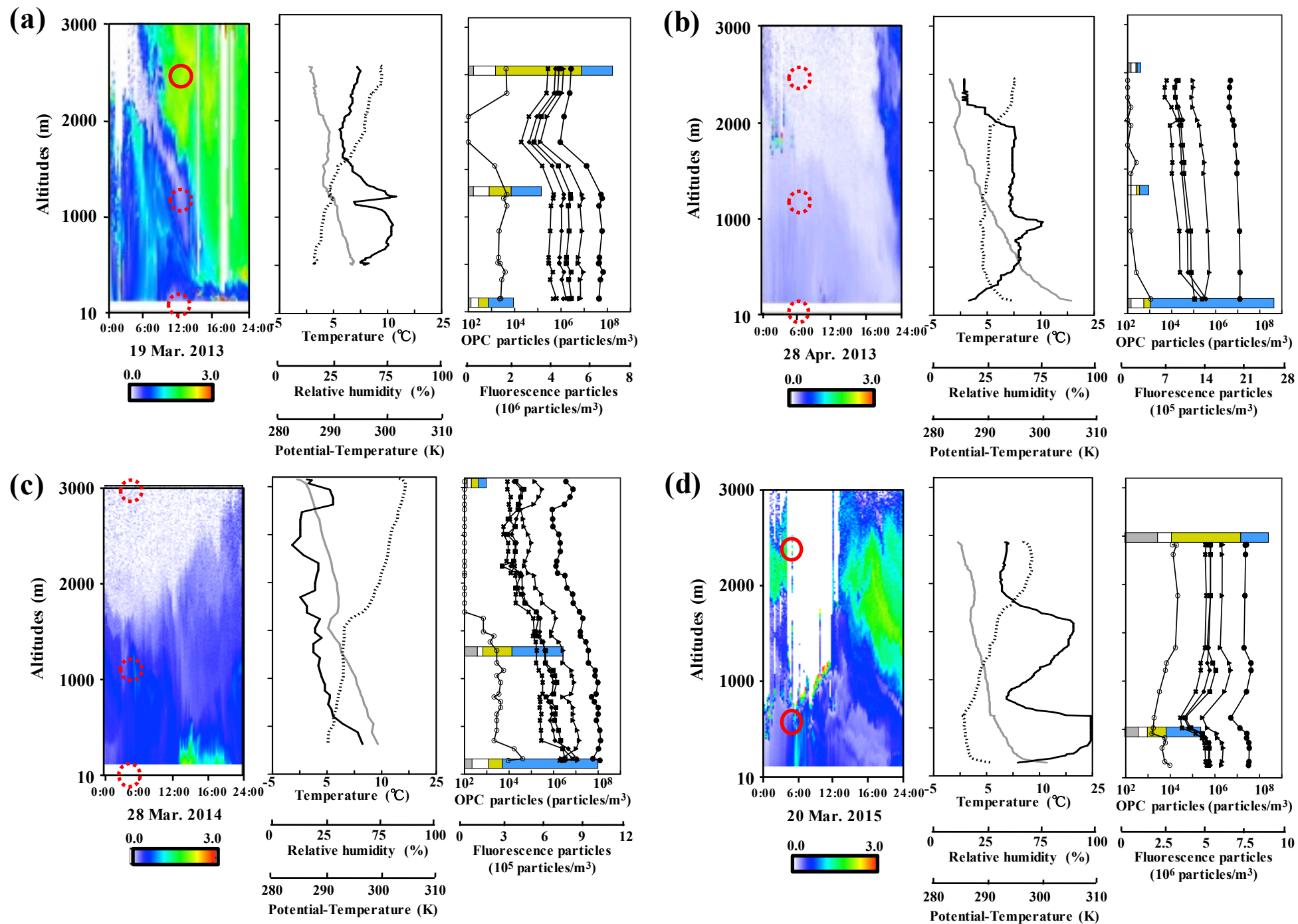
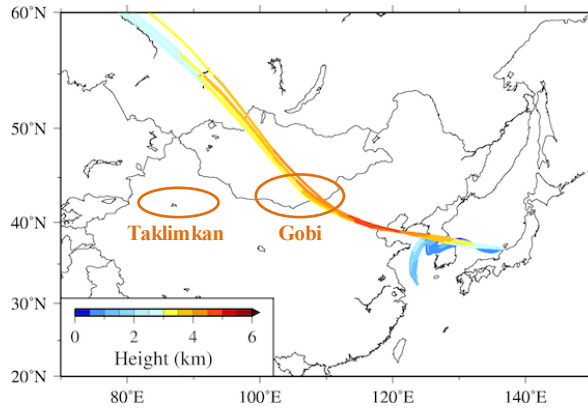
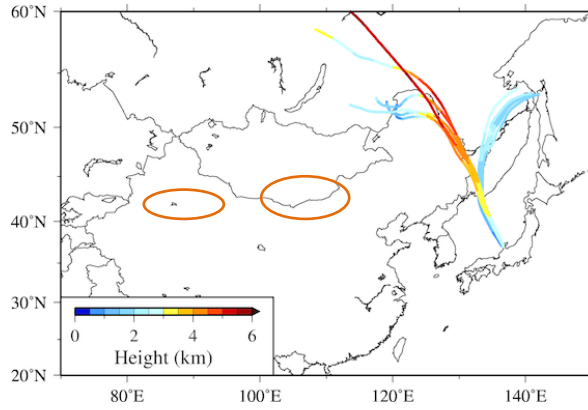


Fig. 2 T. Maki et al.

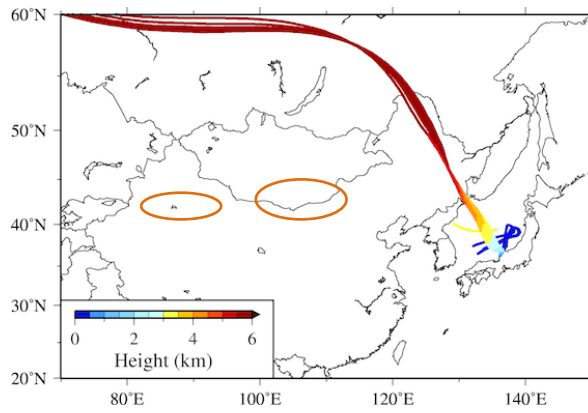
**19 Mar.
2013**



**28 Apr.
2013**



**28 Mar.
2014**



**20 Mar.
2015**

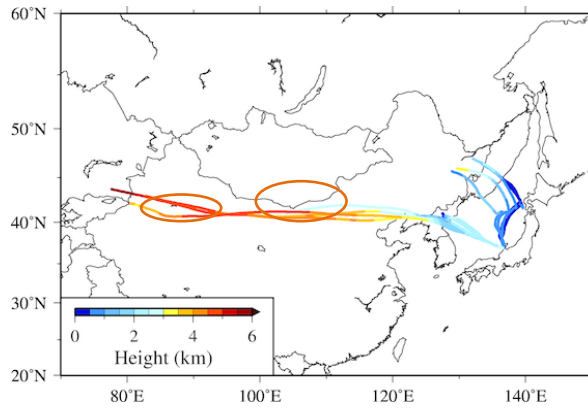


Fig. 3 T.Maki et al.

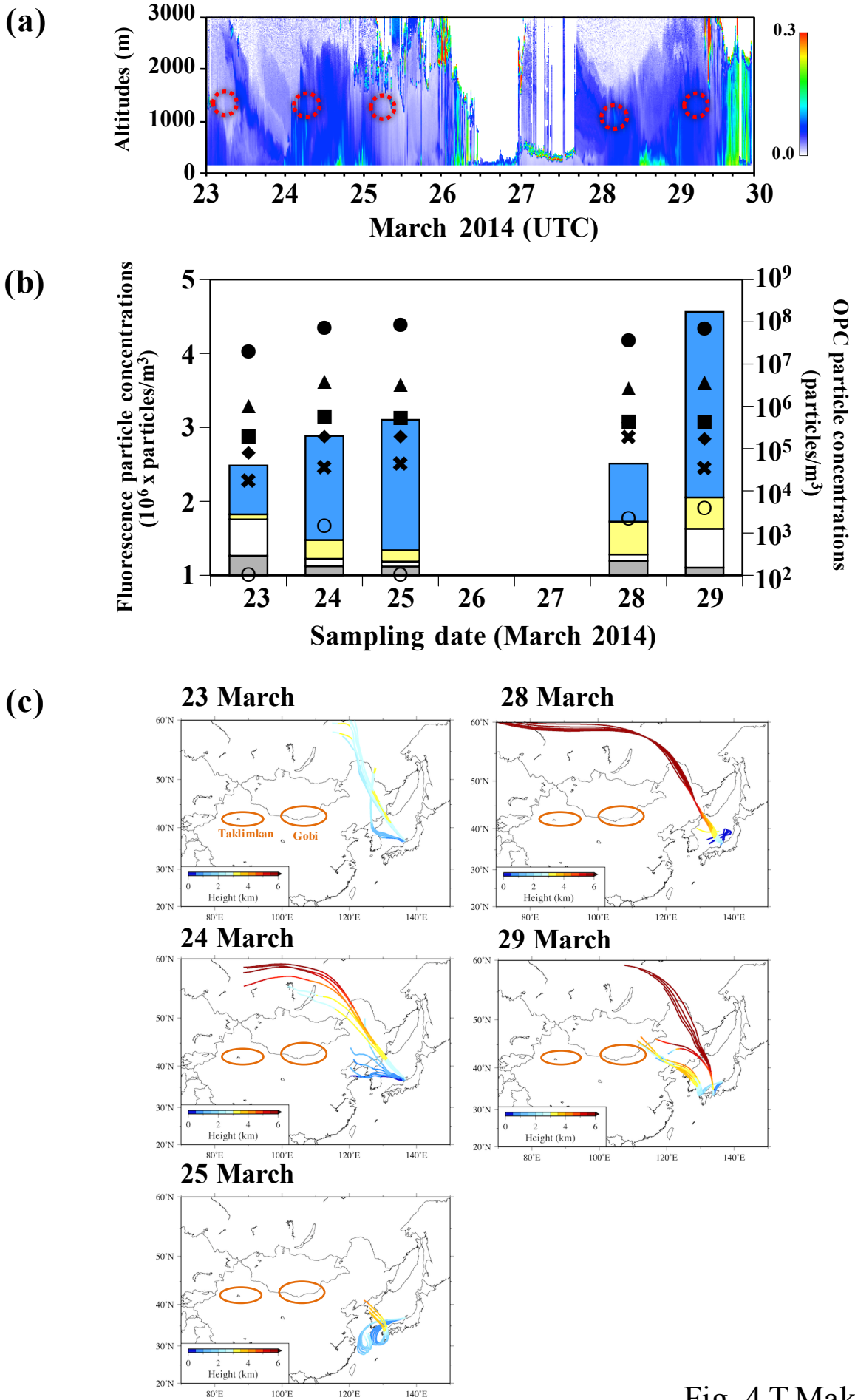


Fig. 4 T.Maki et al.

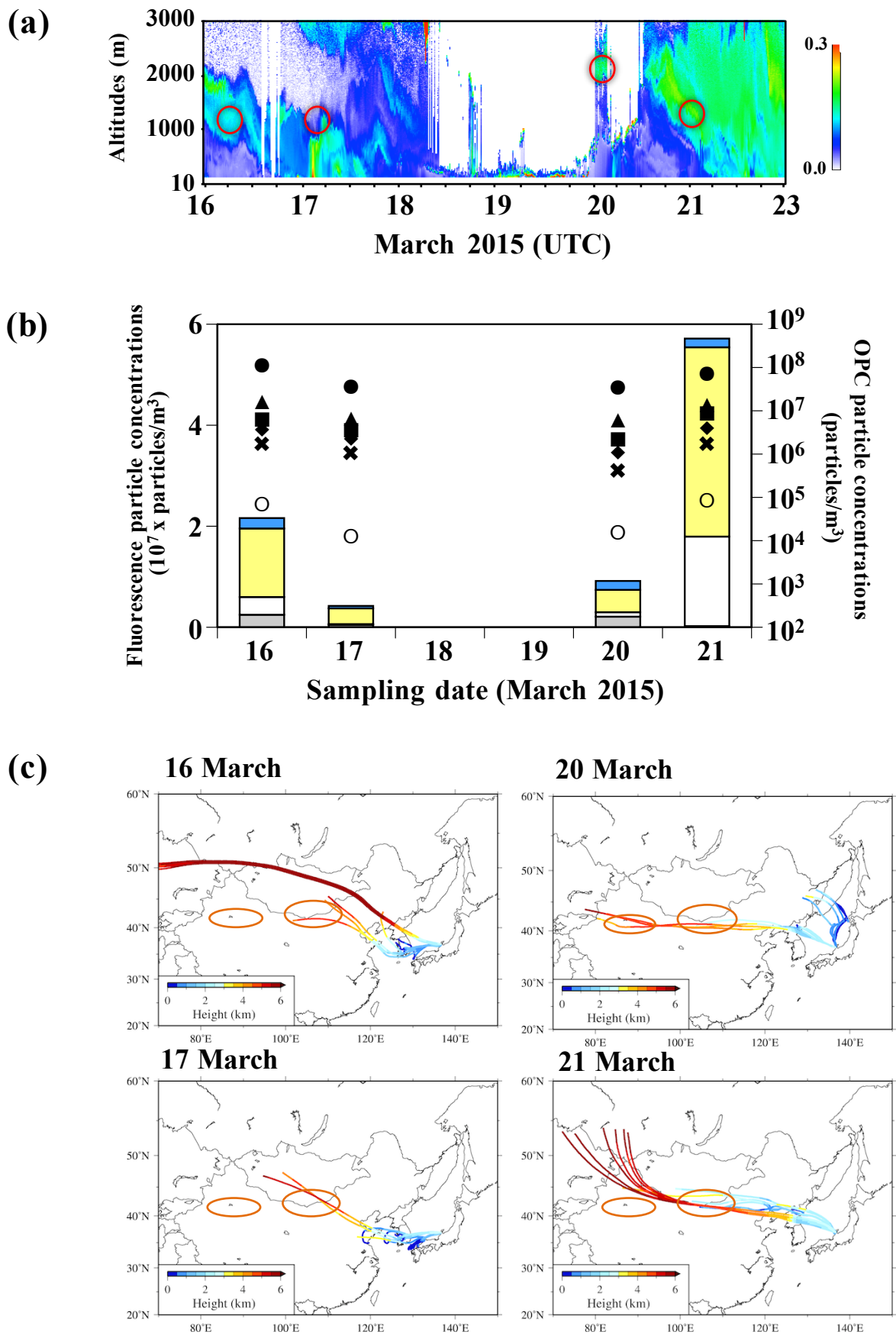


Fig. 5 T.Maki et al.

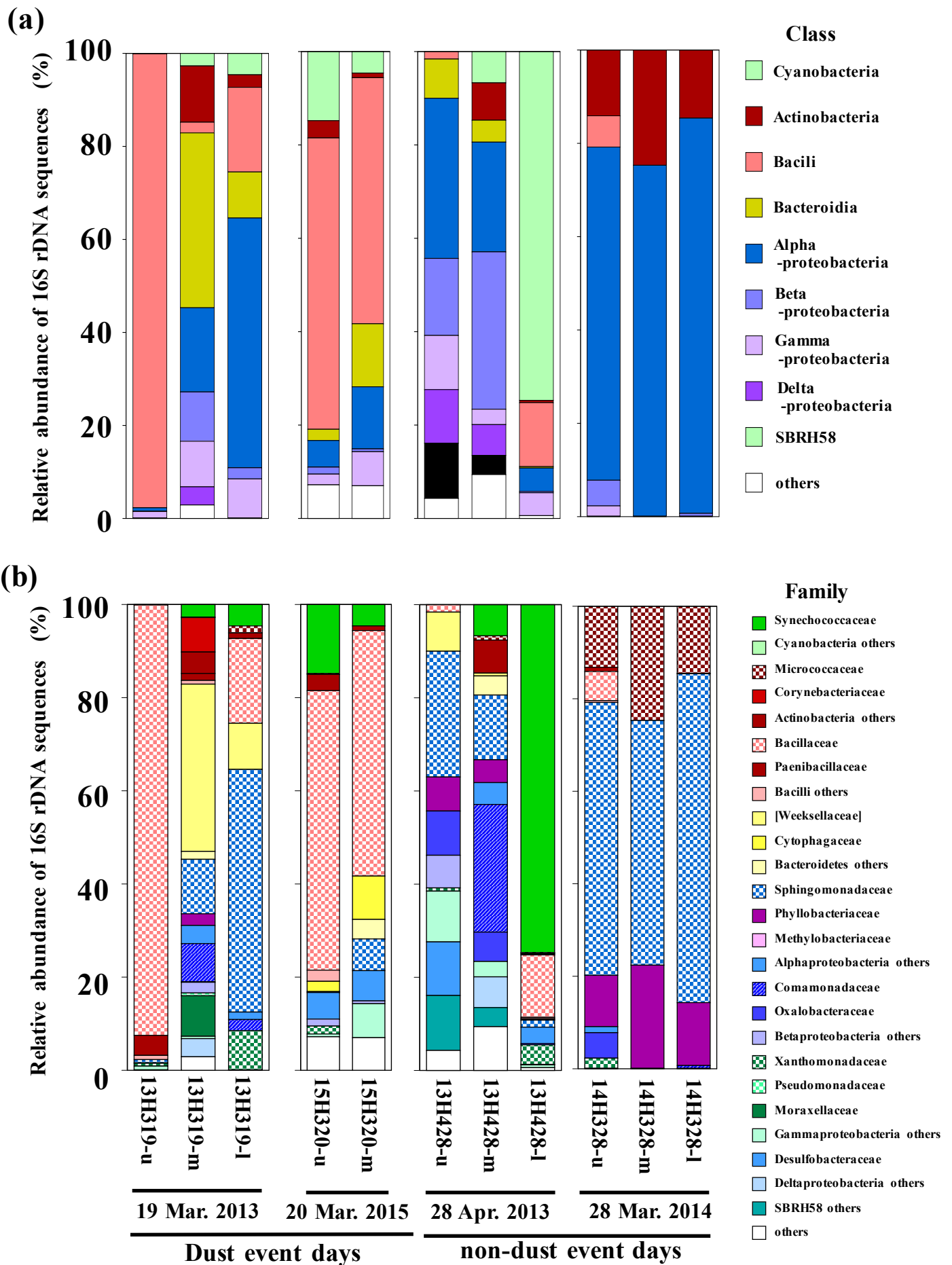


Fig. 6 T.Maki et al.

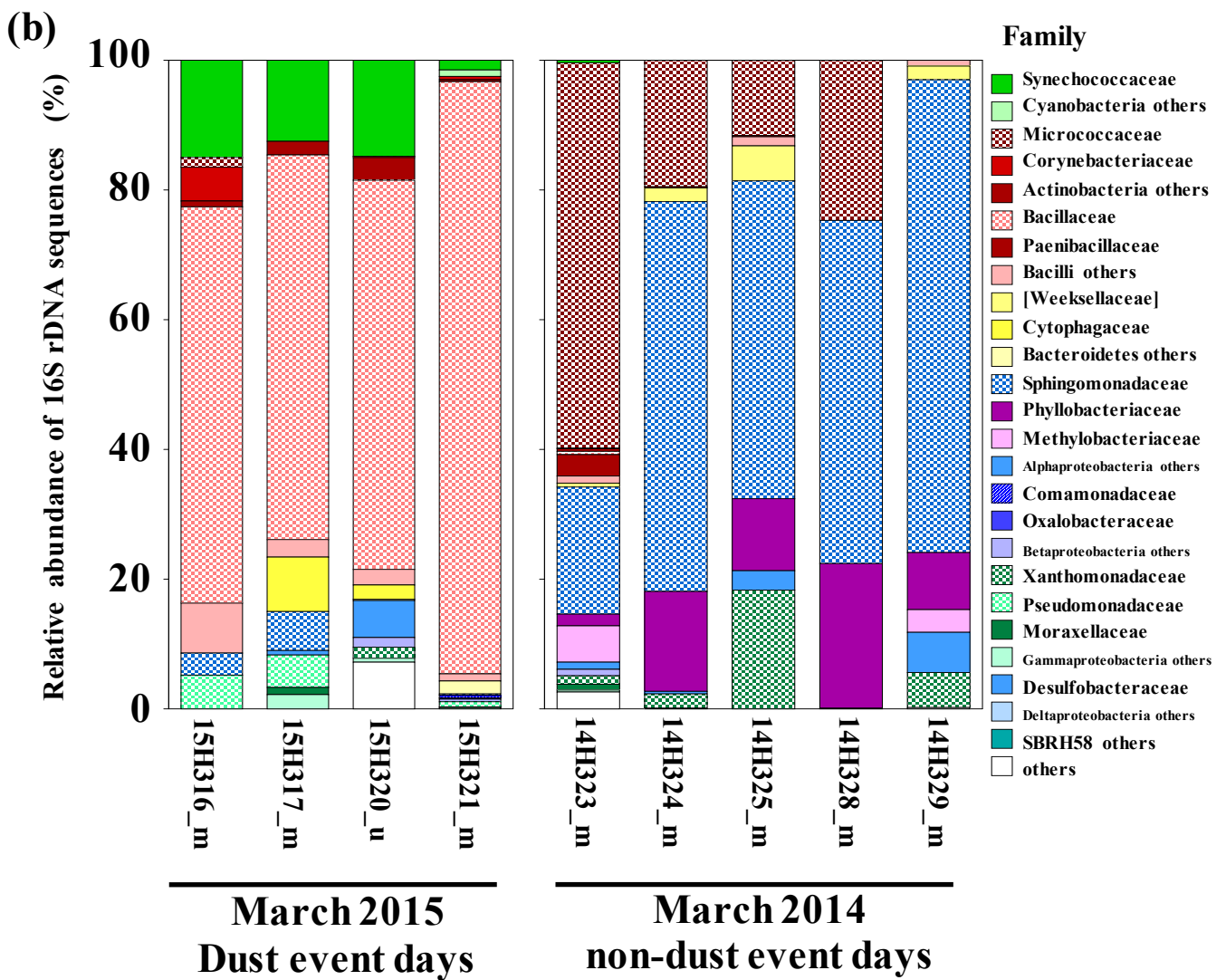
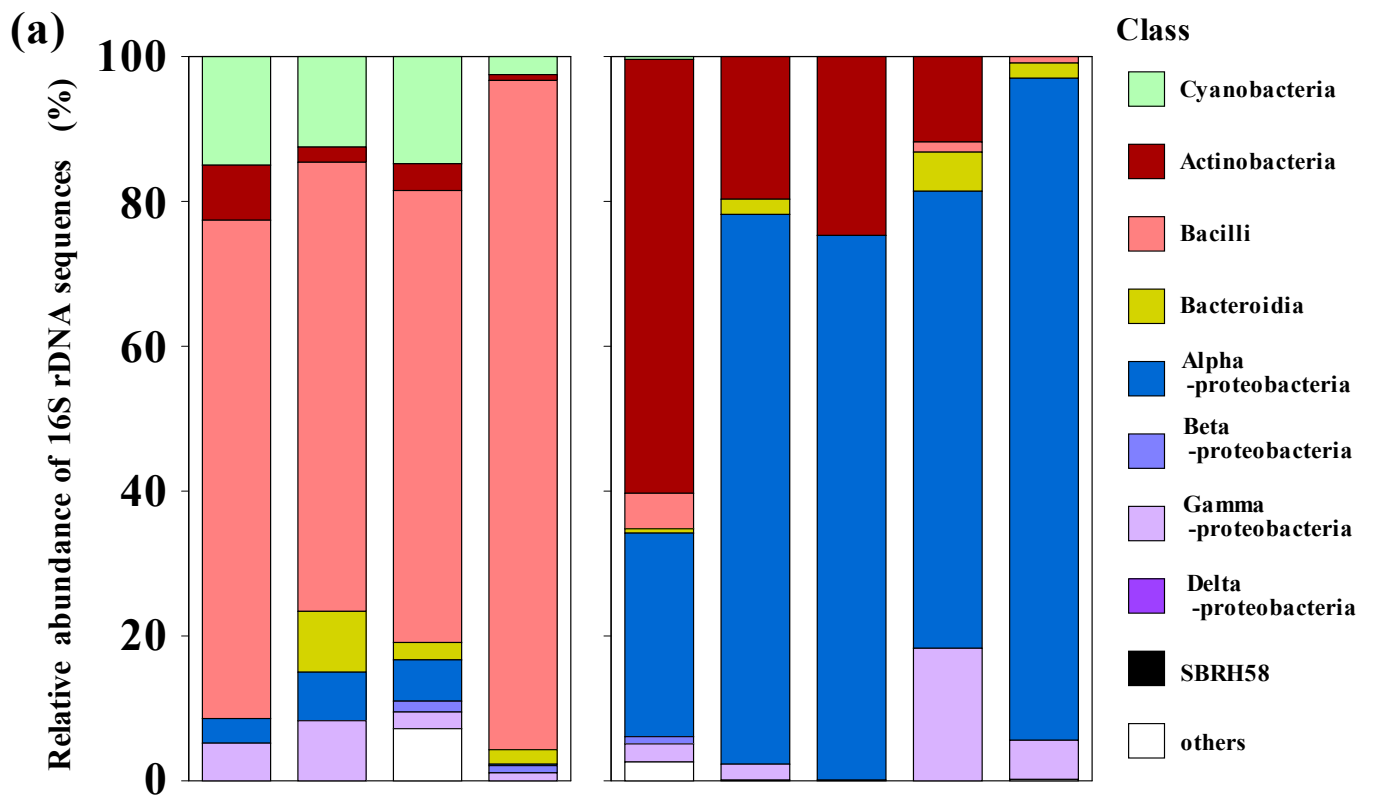
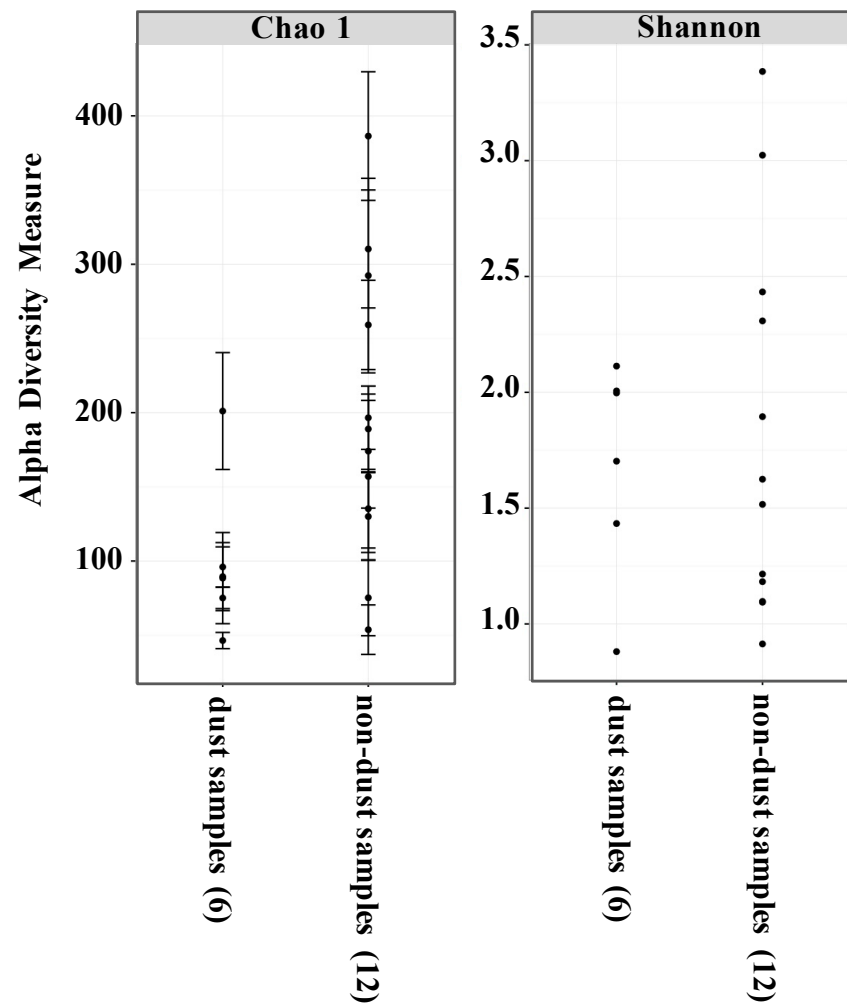


Fig. 7 T.Maki et al.

(a)



(b)

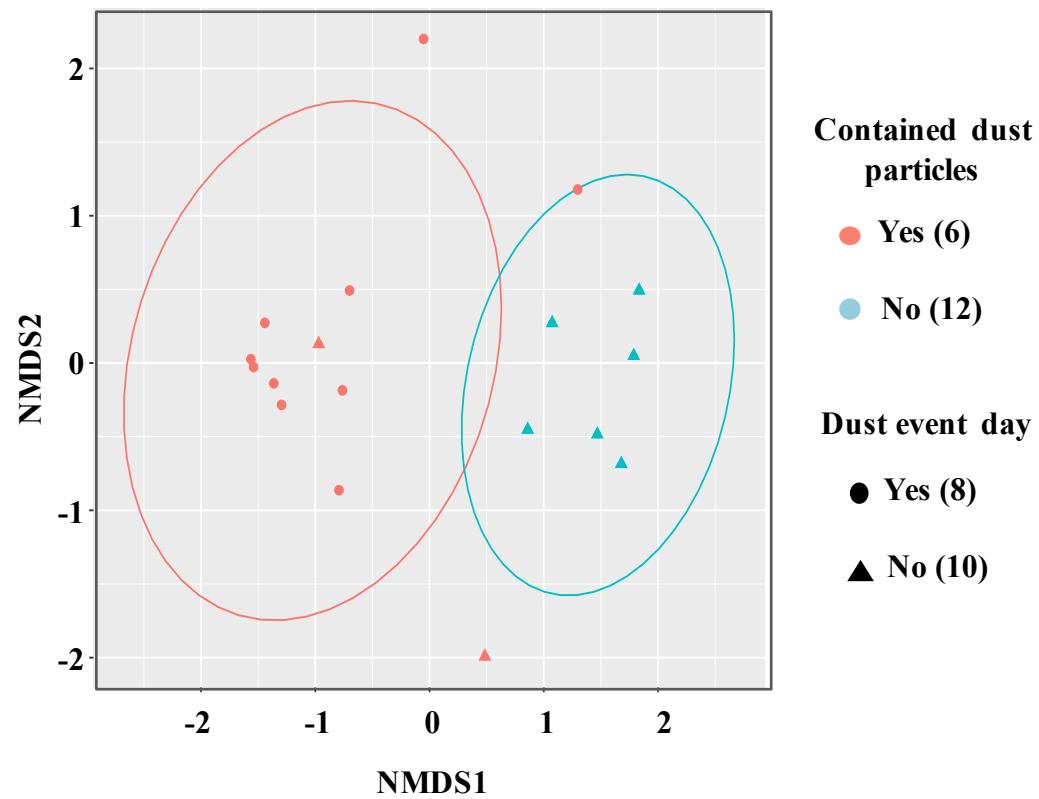


Fig. 8 T. Maki et al.